CHAPTER 3: STRUCTURE OF THE ROCKVALE BLOCK

INTRODUCTION

The Rockvale Block is the most complexly deformed block within the Rockvale - Coffs Harbour region, most of the beds being overturned and showing also at least three s-surfaces recording three deformations on the mesoscopic scale, and presumably the macroscopic scale. However, the macroscopic structures are difficult to recognise because of the uniformity of lithology and absence of distinctive marker horizons. That most of the strata are overturned over such a large area is an intriguing discovery and has been a considerable puzzle to visitors and members of the Department who have been shown the evidence.

It will be demonstrated that the intensity of the deformations increase eastwards from the Girrakool Beds through the Zone of Transitional Schists, the Rampsbeck Schists, the Zone of Migmatites and the Abroi Granodiorite until the rocks are truncated by the Wongwibinda Fault. The western part of the study area is dominated by features produced by D1, but deformations D2 and D3 become progressively more apparent eastwards until most of the D1 structures are unrecognisable.

Several undergraduate students from the Department of Geology, University of New England have written field reports (Geology III Projects) on small areas within the Rockvale Block, but inconsistencies in their results and confusion in the recognition of the various structural elements have made it necessary to completely remap all those areas.

MESOSCOPIC STRUCTURES

Predeformational Structures

PLANAR STRUCTURES

It is possible to recognise lithological differences in outcrops of all metamorphic grades and structure states and it is considered that the ultimate origin of the differences is primary sedimentary bedding. Bedding

which has been deformed by folding, but which has been otherwise little modified, is preserved in the western part of the study area, particularly in the Girrakool Beds (Plate 11F) in which sedimentary structures such as load casts, graded bedding, and groove and flute casts indicate that almost all the strata are overturned, only small isolated areas being upright (right-way-up).

In the more highly deformed eastern part of the block (Wongwibinda Complex) transposition of the bedding has occurred parallel to a penetrative cleavage which grades into a schistosity. Recognition of original So in the highest grade schists is difficult but is occasionally possible where there are alternating colour bands and changes in the proportions of biotite and felsic minerals. Binns (1966) used these criteria to distinguish pelitic and psammitic schists in the Rampsbeck Schists.

LINEAR STRUCTURES

Sole markings such as flute and groove casts occur in the less-metamorphosed beds and have been used to assist in unravelling the structure. On most surfaces the sole marks are sub-parallel, the range in pitch being only 10°, but on one sandy bed at GR 4980 2389 the range in pitch is 80°. Consequently some caution is needed in using these lineations as structural markers.

Structures produced by the first deformation (D1)

PLANAR STRUCTURES

The planar structure imposed by the D1 deformation in the western part of the study area is a slaty cleavage which is penetrative in the pelitic rocks. At some localities it is present in the sandy rocks though more widely spaced than in the pelitic rocks, but at other localities it is weakly developed or non-existent.

Refraction of the cleavage is observed occasionally (Plate 13E). Measurements of the orientations of bedding and cleavage in coarse and fine lithologies (S_1^c, S_1^f) were used to determine the angles between S_1^c, S_1^f and So. Using Snell's Law for the index of refraction,

$n_i \sin_i = n_r \sin_r$, where n_i, n_r are refractive indices of media in which the incident and refracted rays travel,

it has been possible to determine some ratios for n_r/n_i, substituting i for f and r for c.

Sample	$S_1^c \wedge S_1^f$	So $\wedge$ S_1^c	So $\wedge$ S_1^f	$^{nc}/_{nf}$
1	23°	44°	20°	1.31
2	36°	80°	45°	4.07
3	21°	53°	34°	1.38
4	25°	68°	45°	1.89

In future work this ratio of Nc/Nf might provide a valuable measure of the relative competencies of adjacent lithological types.

Microscopic examination shows that the slaty cleavage is defined by parallelism of white mica and chlorite, with some preferred orientations of relict detrital fragments. The slaty cleavage is normally parallel to the axial surfaces of D1 mesoscopic folds developed in So, fanning being observed only where there is refraction into coarser beds.

Conglomerates have not been found but some coarse-grained greywackes contain up to 30% of intraformational mudstone chips which exhibit a preferred orientation. The minor axes of the chips are normal or subnormal to the slaty cleavage and the major axes form a prominent lineation parallel to the cleavage planes. The apparent shortening of the chips normal to the cleavage and elongation within the cleavage attest to the formation of the slaty cleavage normal to the short axis of the finite strain ellipsoid.

The origin of the planar fabric of the white mica defining the slaty cleavage is probably a syntectonic growth of flakes having their shortest dimension parallel to the axis of maximum compressive stress during the M1 metamorphism (see Appendix I pp.80-82). No evidence was found of sandstone dykes and associated features indicative of tectonic dewatering, and it is considered that the cleavage developed after the rocks were highly compacted.

Cleavage similar to the "fracture" cleavage of the Coffs Harbour Block was not observed, all cleavage having the appearance of a "true" slaty cleavage.

In the lower grade Rampsbeck Schists S_1 is expressed as a slaty cleavage defined by the preferred orientation of biotite which has developed in response to increased metamorphism. S_1 in the higher grade Rampsbeck Schists is a penetrative schistosity because of the increase in grain size with the higher grade of metamorphism. Some segregation of quartz in laminae occurs also in the higher grade schists.

LINEAR STRUCTURES

Linear structures produced by D1 are of two types:

(a) a lineation produced by the intersection of So and S_1. On S_1 it shows as a series of faint bandings due to lithological laminations, and on So it shows as series of fractures. This lineation was not commonly observed and its attitude was more readily determined by stereographic plots of So and S_1 measured in the same small area;

(b) a lineation formed by the compaction and elongation of intraformational mudstone chips as described earlier (p.57).

MESOSCOPIC FOLDS

Countless D1 mesoscopic folds occur, particularly in the western part of the field area around Rockvale. Further to the east in the Wongwibinda Complex bedding is rarely recognisable and consequently folds in So are not observed. Typical examples of D1 mesoscopic folds are shown in Plate 11 (A-E). In many cases it is difficult to see the full form of the fold because of poor outcrop, but both symmetrical and asymmetrical types occur. The fold hinges can be either zones of constant curvature or linear features at lines of greatest curvature. In most cases the hinges are rectilinear although some are curved. Angular folds are extremely rare, most having rounded hinge zones. The axial surfaces often seem to be planar in small exposures but are often seen to be curved where several layers in a stock are exposed. The mesoscopic folds are cylindrical (or cylindroidal) over the scale of the outcrop and conical folds have not been observed. However the geometry is often more complex in other ways. In the profile plane the shape of the folded layers is commonly different in adjacent layers, and there is often thickening of the hinge region and thinning of the limbs.

A wide range of fold sizes occur from almost microscopic (λ = 1 cm) to the folds observed in Balaclava Stream (GR 4957 2390) with λ = 20 m. The dimensions of several surfaces of the folds illustrated in Figure 42 are listed in Table 6. The range of interlimb angles is from about 150° to 0° (isoclinal) and is not systematic in a regional sense but be found in one outcrop (for example the "Double Fold Locality", much studied by undergraduates, Figure 51). Even in one fold (Fig. 42C) a progressive change from 58° to 36° in different layers has been recorded.

Within one fold the half-fold length (f), and the amplitude can also

PLATE 11

D1 Mesoscopic Structures from the Rockvale Block

A. Mesoscopic fold with a narrow hinge zone which is rounded. Dip isogons, stack inflection surfaces and train inflection surfaces for this fold are illustrated in Figure 42 A and B. Pen for scale is 0.13m long.

B. Fold in sandstone layer with slight thickening in the hinge zone. Pencil for scale is 0.14m long.

C. Gentle mesoscopic fold in siltstone layers. Hinge area is wider than that illustrated in Plate 11A. Pencil is 0.14m long.

D. Fold in sandstone layers showing displacement of the trace of the axial surface by a mesoscopic fault running across centre of photograph. Fold axes are steeply plunging. Same scale as for Plate 11A.

E. Rounded fold being affected by the D2 episode of deformation. Plunge of fold axis changes along the fold from gently plunging towards the southeast, through horizontal to gently plunging towards the northwest. Direction of north is towards left hand side of page. Scale same as for Plate 11A.

F. Series of graded beds with base of silt grading upwards to mud, indicating the sequence is overturned. A penetrative cleavage in the mud cuts the bedding at an angle of approximately 15°, but is not developed to any marked extent in the silty portion of the bed. Photograph covers an area of approximately $1m^2$.

All photographs in this plate were taken in the vicinity of the Double Fold Locality on Rockvale Creek (GR 4981 2405).

A

B

C

D

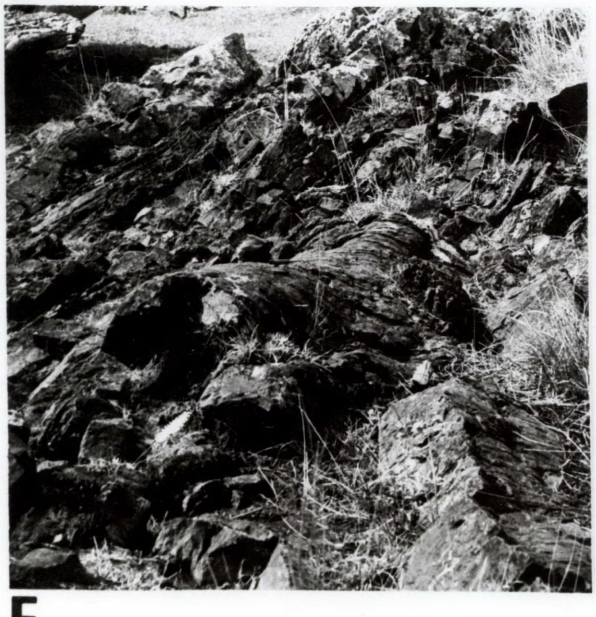

E

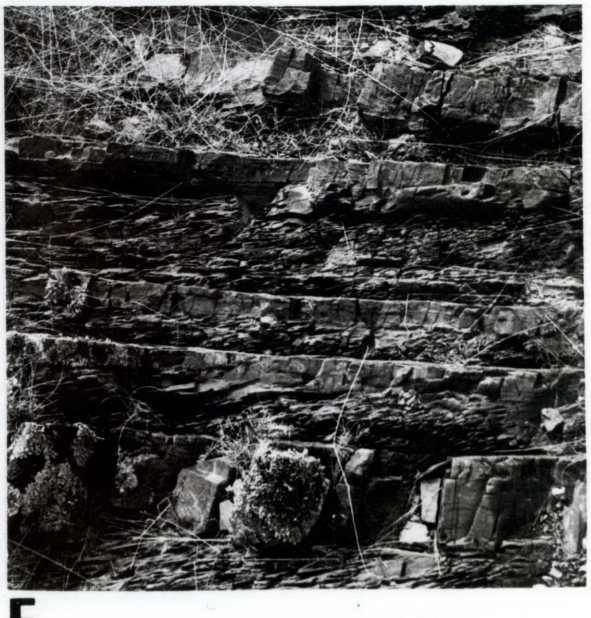

F

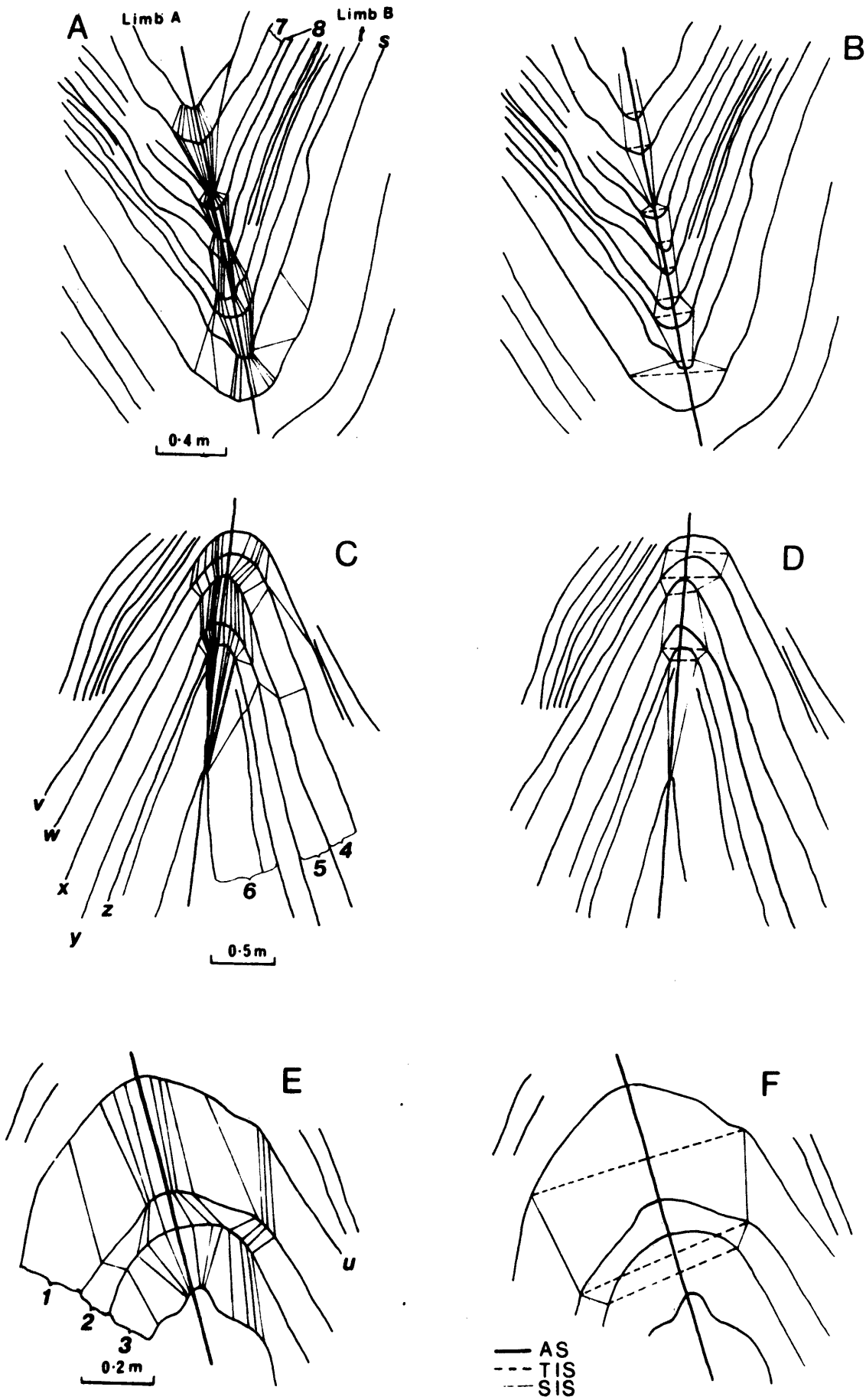

Fig. 42: Dip isogon and inflection surface patterns for D1 folds from the Rockvale Block.

Table 6; Dimensional data for D1 and D2 mesoscopic folds from the Rockvale Block
Values of c, f, λ, A and V are given in metres, θ in degrees and V in percent.

	Fold	Folded Surface	θ	c	f	λ	A	V	c/f	λ/L	A/L	A/λ	Z	Z/L
D1 mesoscopic folds	Fig.42 Fold A	s	55	0.54	2.40	2.68	0.93	44	0.23	0.56	0.19	0.35	0.77	0.16
		t	58	0.10	2.00	2.02	0.85	50	0.05	0.51	0.21	0.42	0.82	0.21
	Fig.42 Fold E	u	110	0.32	1.50	2.53	0.38	15	0.21	0.85	0.13	0.15	0.33	0.11
	Fig.42 Fold C	v	58	0.60	3.60	3.98	1.43	45	0.17	0.55	0.20	0.36	1.26	0.17
		w	52	0.54	3.90	3.91	1.62	50	0.14	0.50	0.21	0.41	1.45	0.19
		x	47	0.42	4.25	3.82	1.85	55	0.10	0.45	0.22	0.48	1.75	0.21
		y	40	0.45	4.50	3.59	2.01	60	0.10	0.40	0.22	0.56	1.85	0.21
		z	36	0.24	5.04	3.62	2.33	67	0.05	0.36	0.22	0.64	2.42	0.22
D2 mesoscopic folds	Fig.46 Fold E	a	135	0.20	0.60	1.13	0.10	6	0.33	0.94	0.08	0.08	0.08	0.06
		b	135	0.11	0.61	1.14	0.11	7	0.18	0.93	0.09	0.09	0.10	0.08
		c	120	0.13	0.60	1.06	0.12	11	0.22	0.89	0.10	0.11	0.12	0.10
		d	113	0.20	0.58	1.01	0.13	13	0.34	0.87	0.11	0.13	0.10	0.09
	Fig.46 Fold C	e	85	0.02	0.03	0.050	0.007	16	0.67	0.84	0.12	0.14	0.028	0.05
		f	74	0.015	0.04	0.054	0.012	28	0.41	0.72	0.16	0.22	0.078	0.11
		g	68	0.012	0.06	0.070	0.020	37	0.22	0.63	0.18	0.29	0.17	0.15
	Fig.46 Fold A	h	30	0.004	0.09	0.054	0.044	71	0.04	0.29	0.24	0.82	0.43	0.23
		i	40	0.006	0.09	0.070	0.041	62	0.07	0.38	0.23	0.60	0.39	0.24

vary markedly (for example Fold C, Table 6 and Fig. 42). However the ratio A/L is remarkably consistent and so also is the wavelength although for this fold the λ/L ratio is also variable. Migration paths of λ/L and A/L plotted against θ (Fig. 43) for Fold A of Fig. 42 intersect those for Fold C. These paths contrast with those of folds in the Redbank River Beds (Fig. 19) which fall in a tight cluster regardless of size.

Chord ratios range from 0.05 to 0.23 indicating that the folds are of rounded (paraboloidal) type. However those with c/f of 0.05 do approximate closely to angular folds. For the folded surfaces V to Z the A/λ ratio changes from 0.36 to 0.64 indicating that from surface V to surface Z the fold is becoming progressively more flattened. This is also reflected in ther percent shortening (V) which changes from 45 to 67%.

Patterns of dip isogons and graphs of T and t versus α (Figs. 42 and 44) show that all three of the fold classes of Ramsay (1967) are represented with some layers containing elements of more than one class (e.g. Layer 8, class 1C-2-3). Fold E equates with a parallel fold which has been modified by some flattening (see Layer 1) whereas layer 5 of fold C equates with Class 2 (similar folds). Some layers (e.g. 7, part of 2) have a class 3 geometry. It seems that the more competent layers have a class 1 to class 2 shape and the more incompetent layers equate with class 3. The D1 folds have been influenced by a later period of folding (D2) which might have modified the shapes slightly to produce the complex patterns outlined above.

Fold train and fold stack inflection surfaces have been constructed (Fig. 42) and values of Z and Z/L calculated (Table 6). The values of Z/L range from 0.11 to 0.22 and are relatively consistent for the surfaces in the stack in Fold C (0.17 to 0.22). The TIS $\wedge$ AS is approximately 90° and SIS $\wedge$ AS (ϕ) change from being 0° for some layers to as much as 65° for other layers. These values are approximately those of class 1 and class 2 folds.

D2 Mesoscopic Structures

Mesoscopic structures produced by the D2 deformation become more abundant in the eastern part of the Rockvale Block. In the Girrakool Beds this deformation is represented mainly by kink bands in the S_1 cleavage but in the upper reaches of Boundary Creek chevron folds occur. Towards the east S_1 becomes intensely folded and is frequently transposed into S_2.

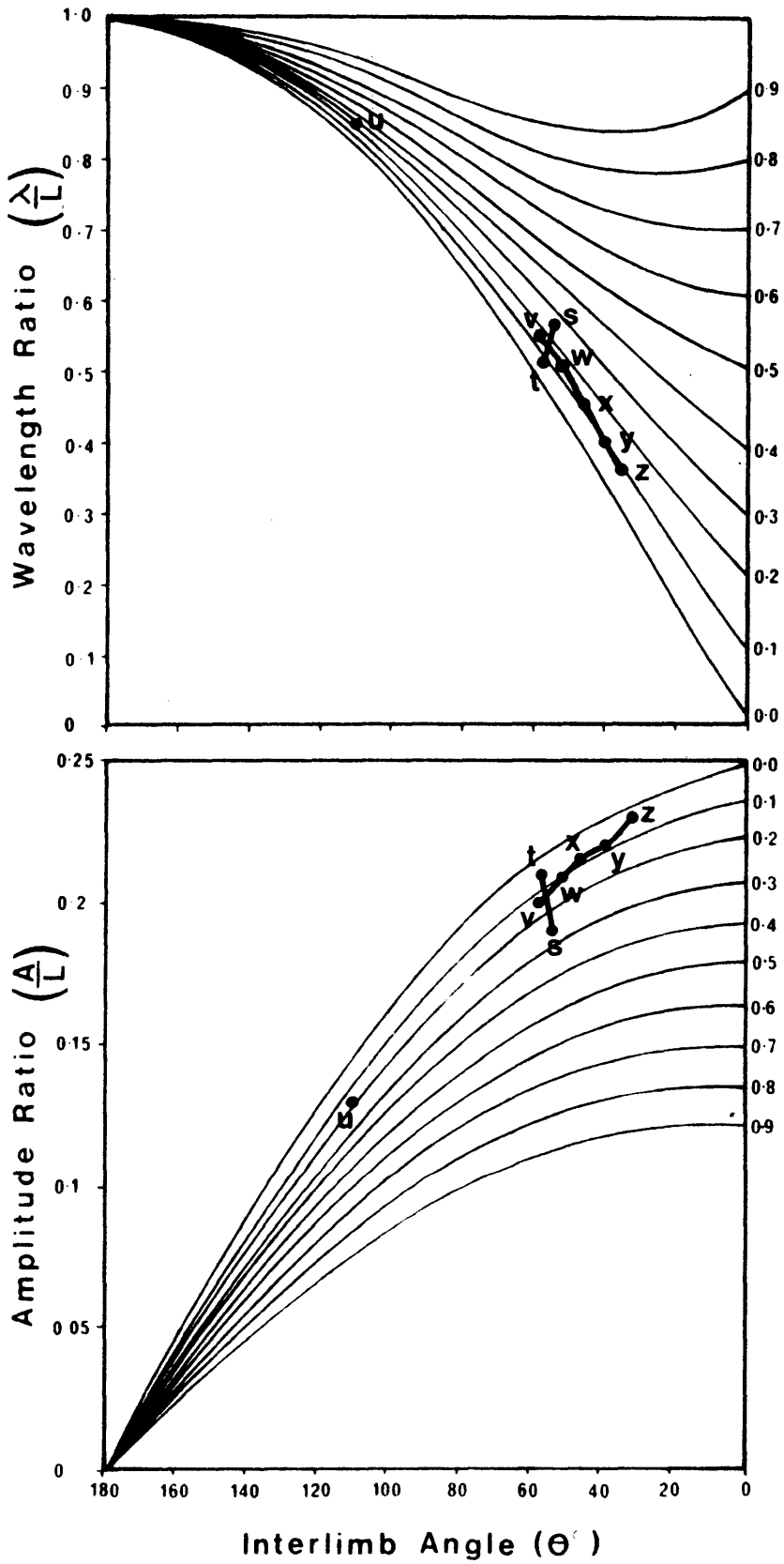

Fig. 43: $\frac{\lambda}{L}$ and $\frac{A}{L}$ versus θ graphs showing migration paths of folded surfaces for D1 mesoscopic folds from the Rockvale Block.

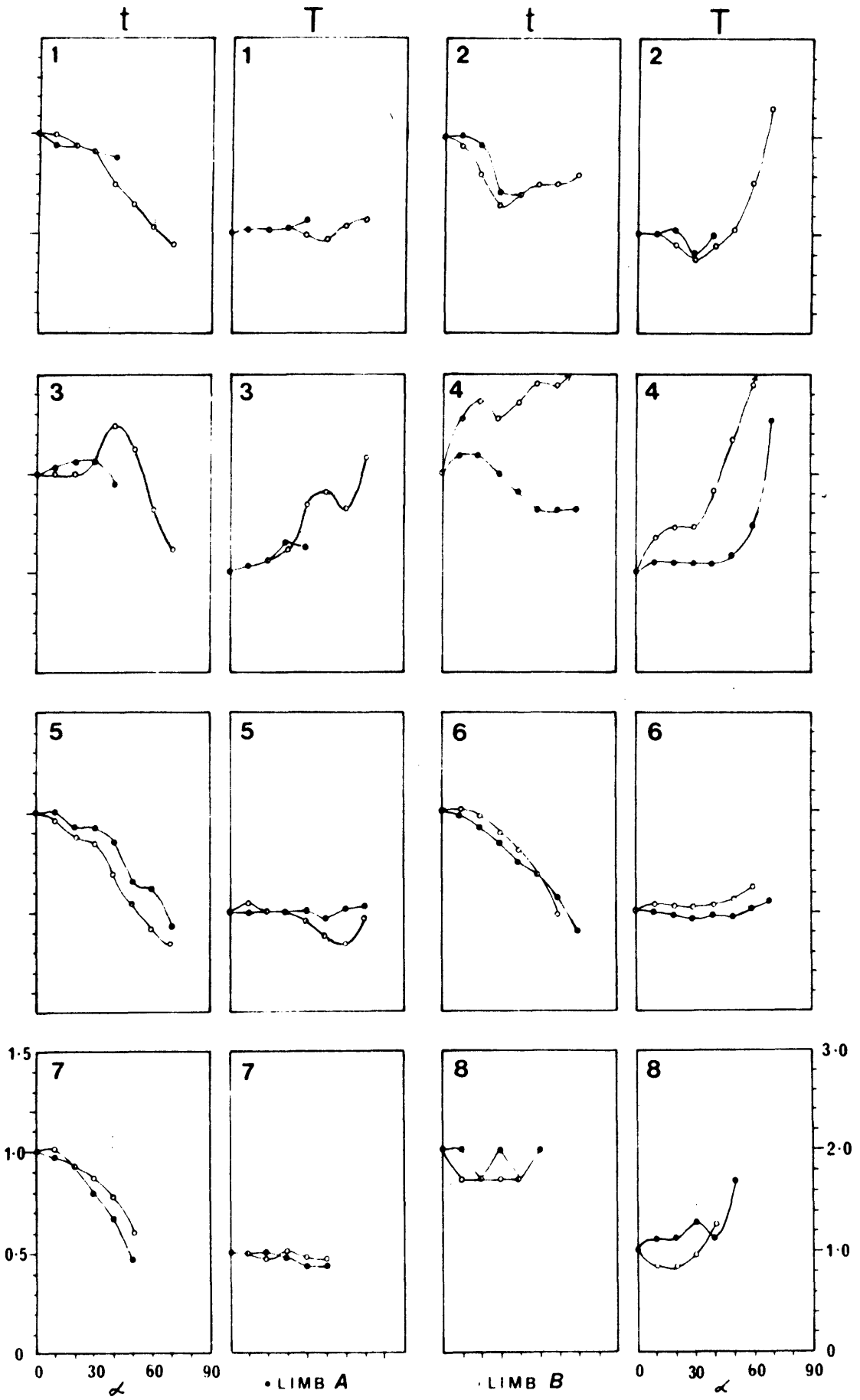

Fig. 44: Graphs of T and t compared with α for D1 mesoscopic folds from the Rockvale Block.

PLANAR STRUCTURES

In the western part of the field area D2 planar structures are expressed as axial surfaces to the kink bands and chevron folds produced by D2. For many folds concomitant fracturing of the axial surface has occurred to produce an axial surface crenulation cleavage (S2). Some minor movement parallel to the S_2 surface has occurred displacing the S_1 surface in areas where deformation by S_2 has been relatively intense. The spacing between S_2 ranges from 1 cm to 30 cm and is not penetrative on the scale of the outcrop.

It is not until the higher grade Rampsbeck Schists are reached that S_2 becomes common and is similar to S_1 in that it occurs as a schistosity, in this case axial plane to the D2 folds. S_2 also occurs as a penetrative schistosity in some localities with S_1 being transposed into S_2.

In some outcrops S_1 is intensely folded with a constant axial surface S_2 (e.g. GR 5195 2500 where quartz segregations produced by D1 have been isoclinally folded and partial transposition into S_2 has taken place, Fig. 45). In other outcrops S_1 has been completely transposed into S_2, which parallels the axial surfaces of the relict folds in S_1. Recognition of the production of S_2 by transposition of S_1 is indicated by the survival of small tightly appressed fold hinges. S_2 forming axial surfaces to S_1 folds, and transposition of S_1 to S_2 have been recorded in the same outcrop by Fisher (1968) from the Little Chandler River area (GR 5176 2470). In most cases the transposition has only reached stage 3 of Turner and Weiss (1963, p.93) where the attunated limbs of folds in S_1 are being replaced by slip surfaces parallel to S_2.

LINEAR STRUCTURES

The lineation produced during D2 results mainly from the intersection of S_2 and S_1. Lineations produced by the intersection of So and S_2 were not observed. $L(S_1 \times S_2)$ occur as closely spaced parallel striations on S_1 surfaces and where transposition has taken place the lineation is seen as faint colour bandings in S_1. This lineation is parallel to fold axes $B_{S_1}^{S_2}$.

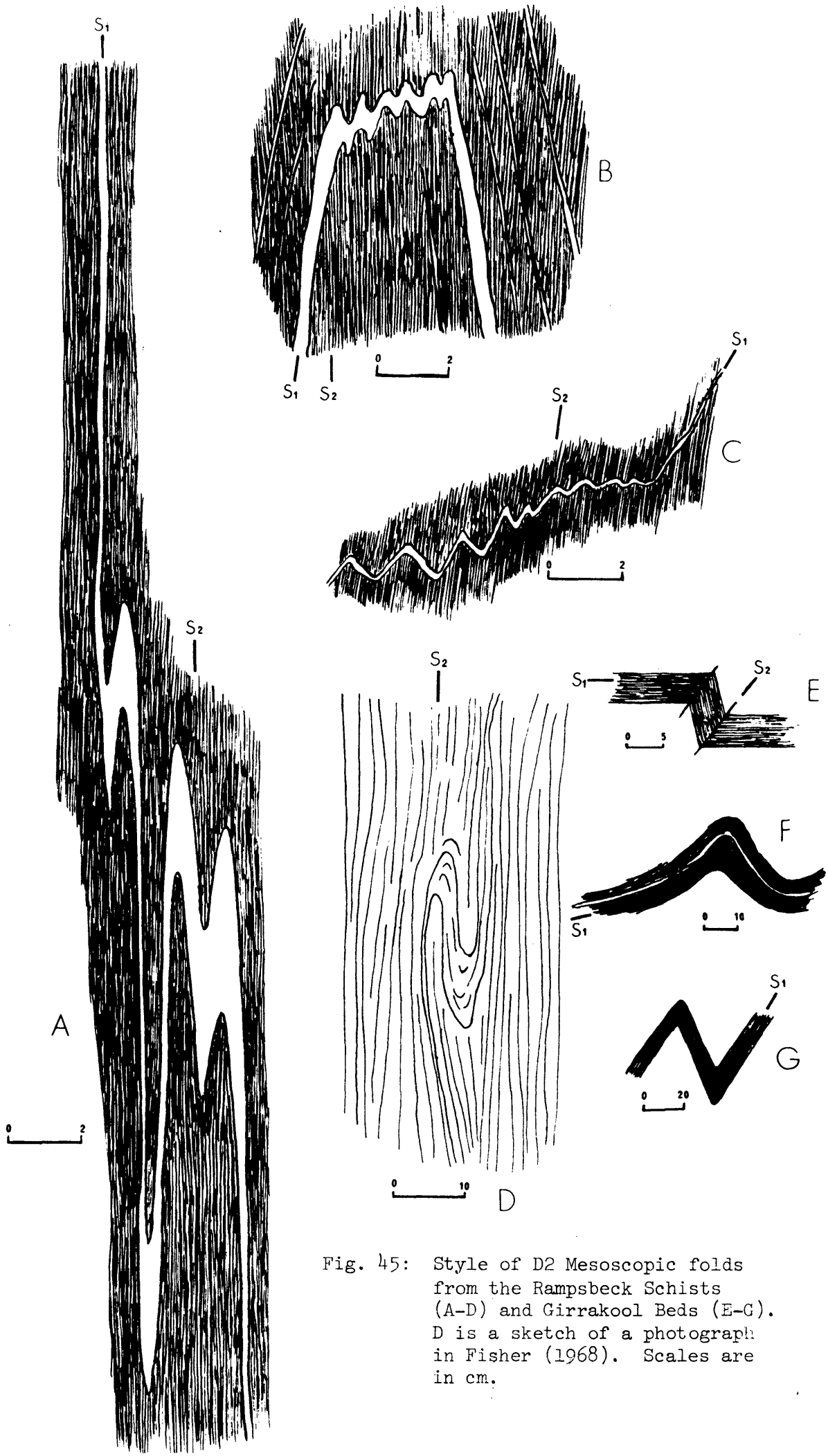

Fig. 45: Style of D2 Mesoscopic folds from the Rampsbeck Schists (A-D) and Girrakool Beds (E-G). D is a sketch of a photograph in Fisher (1968). Scales are in cm.

MESOSCOPIC FOLDS

The style of D2 mesoscopic folds varies from slight flexures, kink bands and chevron folds in the Girrakool Beds to isoclinal folds in the high grade Rampsbeck Schists (Fig. 45A - G, Plate 12). Quartz veins parallel to S_1 have been deformed and the material has migrated into the hinge zones of the B_1^2 folds (e.g. Fig. 45A, F). The folds are cylindrical over the scale of the outcrops.

The D2 folds vary from symmetrical chevron folds (Fig. 45G, Plate 12, 13) to asymmetrical isoclinal folds with the limbs being markedly different in length (Fig. 45A). The folds are usually smaller than those produced by D1, ranging in size from the microscopic scale up to amplitudes of about 1.5 m. Dimensional data calculated from formulae in Chapter 1 (pp. 10-14) are listed in Table 6 for individual surfaces of three representative D2 folds in deformed S_1 from the Girrakool Beds. Interlimb angles (θ) are extremely variable (range 30° to 135°) and no systematic change was observed. In fact, in the space of 100 m in the upper reaches of Boundary Creek D2 folds were observed with interlimb angles ranging from 42° to 134°.

Within a fold stack the folded surfaces exhibit approximately the same amplitudes and wavelengths and consequently λ/L and A/L are consistent. Migration paths for A/L and λ/L versus θ (Fig. 47) indicate that these D2 folds occupy a large field on these graphs and appear to be not as restricted as those of D1 folds (Fig. 43) although when more dimensions for folds are determined the picture may become clearer.

The chord ratio ranges from 0.04 to 0.67 indicating that all the surfaces are rounded (paraboloidal) folds verging towards angular folds for those with a chord ratio of less than 0.1.

The A/λ ratio remains relatively constant for fold A (Fig. 46, Table 6) with the percent shortening (V) changing from 5.9% to 12.6% for adjacent layers. There is a change in the A/λ ratio from 0.14 to 0.29 for Fold C (Fig. 46) and a consequent change in V from 16.4% to 36.6% and for fold A, A/λ = 0.60 and 0.82 and V = 62.0% and 71.4% indicating that from folded surface a to g then i and h, each surface is becoming progressively more flattened.

Dip isogons (Fig. 46) indicate that convergent and parallel isogons are more common than divergent ones. Graphs of T and t compared

PLATE 12

D2 Mesoscopic Structures from the Rockvale Block

A. Gentle fold produced by flexuring on the limb of a D1 mesoscopic fold at the Double Fold Locality (GR 4981 2405). Hammer indicates scale.

B. Gentle flexuring of the long limb of a D1 asymmetric fold at the Double Fold Locality. Width covered by this photograph is approximately 5m.

C. Dextral kink band in highly cleaved mudstones from the upper reaches of Boundary Creek. Magnification $\times \frac{1}{2}$.

D. Tight chevron folds in the slaty cleavage from Domain 36. Pencil for scale is 0.15m long.

E. Gentle flexuring in widely-spaced cleavage from Domain 36. Hammer indicates scale.

F. Large kink band in widely-spaced cleavage from the same locality as Plate 12E. Hammer indicates scale.

Plates 12C to F were all taken within a distance of 100m along the banks of Boundary Creek west of the Rockvale - Aberfoyle road around GR 5000 2476.

A

B

C

D

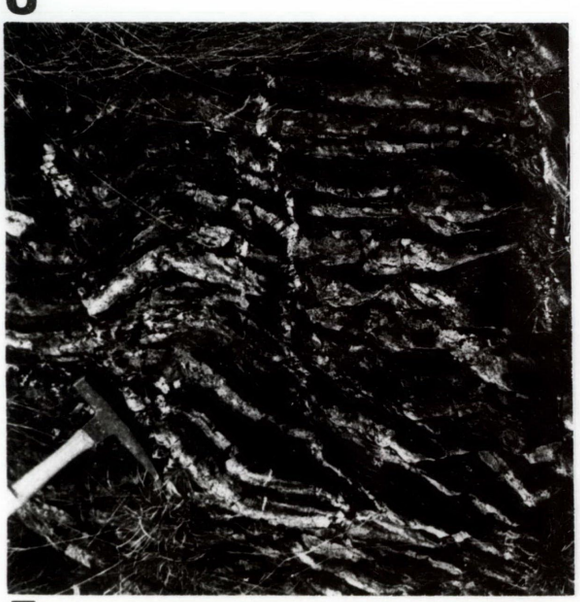

E

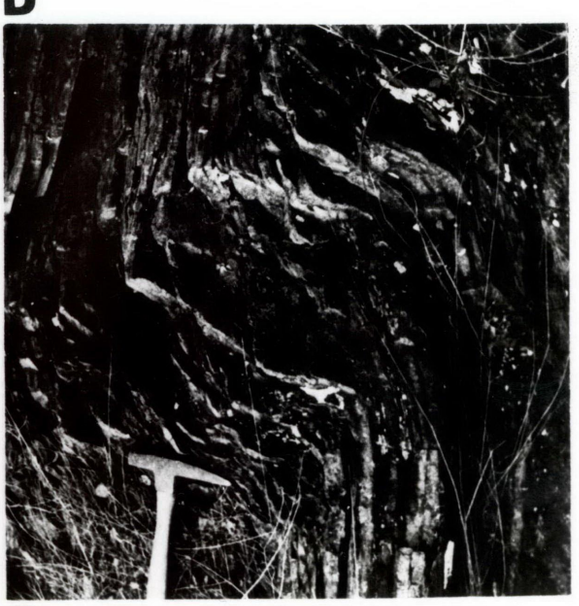

F

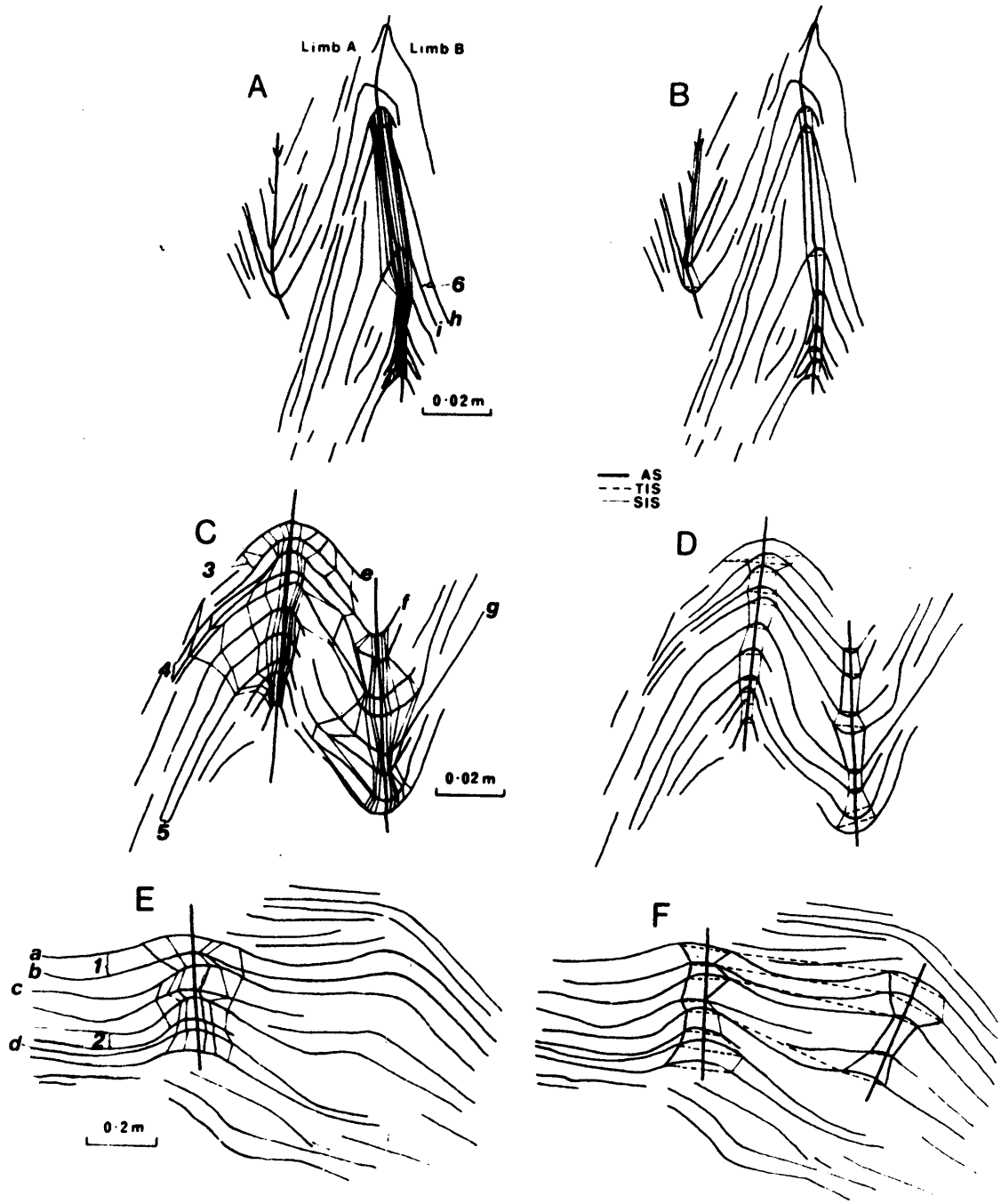

Fig. 46: Dip isogon and inflection surface patterns constructed for mesoscopic D2 folds from the Rockvale Block.

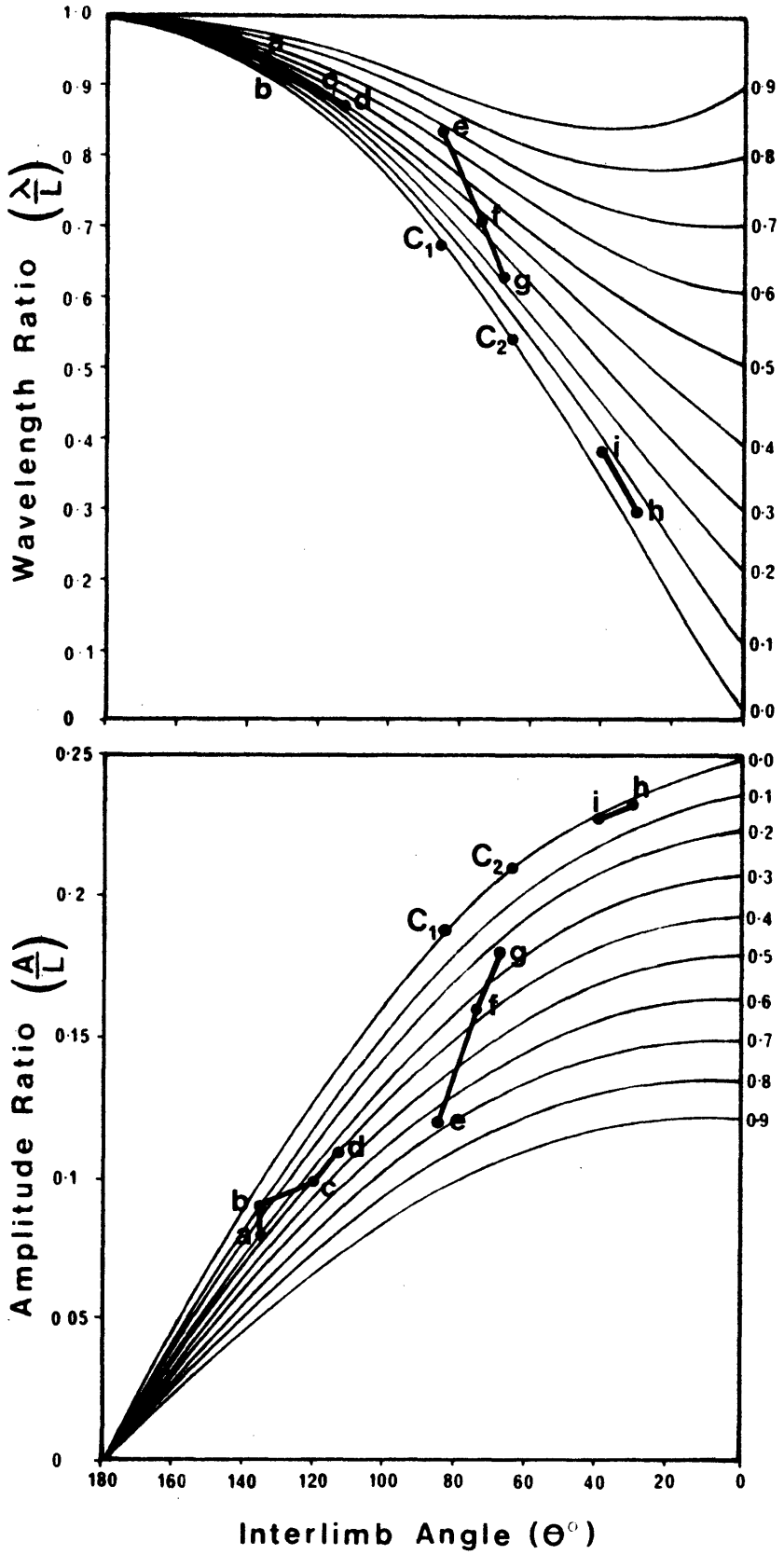

Fig. 47: $\frac{\lambda}{L}$ and $\frac{A}{L}$ versus θ graphs showing migration paths of folded surfaces for D2 mesoscopic folds from the Rockvale Block.

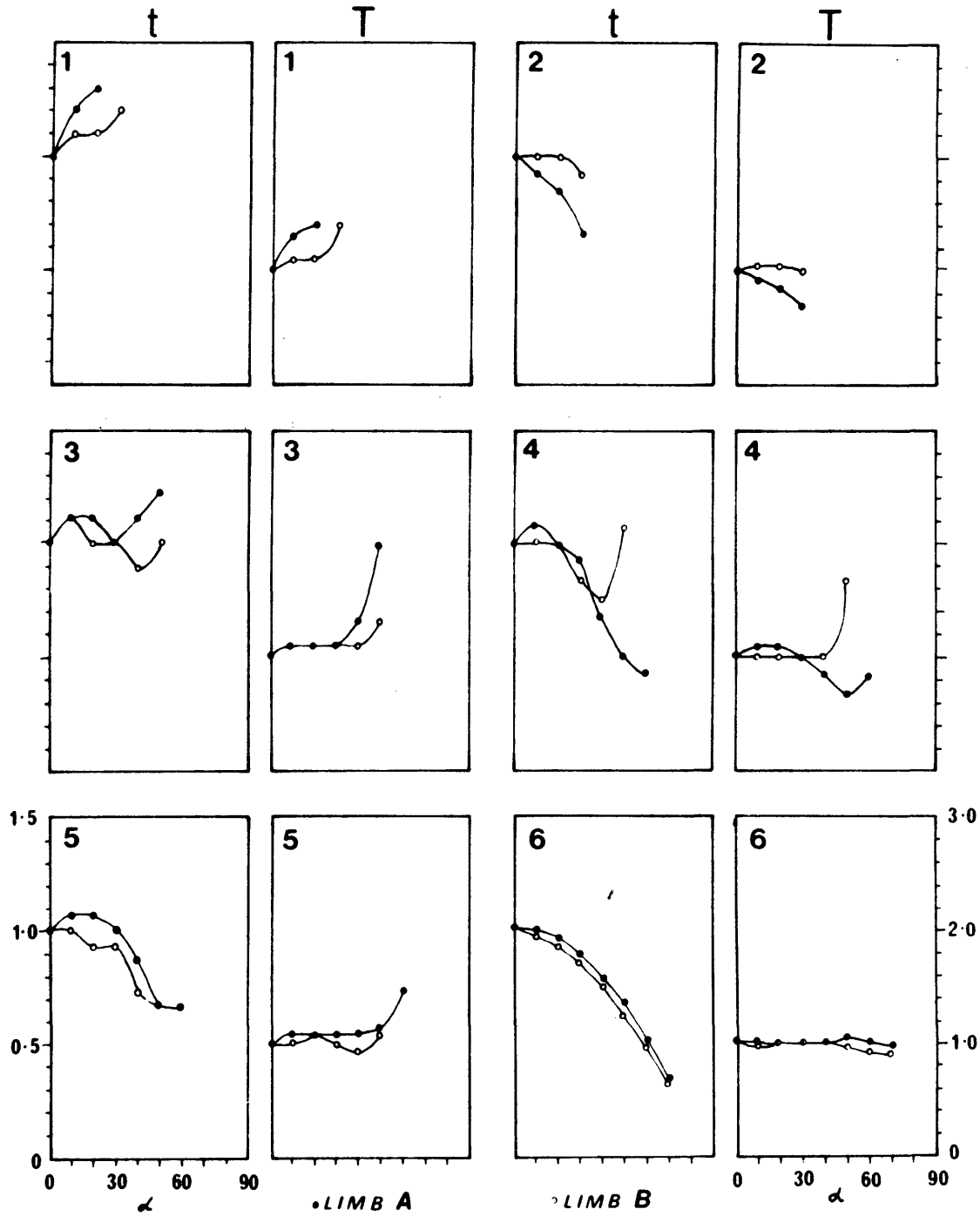

Fig. 48: Graphs of T and t compared with α for D2 mesoscopic folds from the Rockvale Block.

with α (Fig. 48) indicate that most layers measured on Figure 46 (1, 3, 4, 5) approximate to class 1A with minor influence to the pattern by other classes, particularly class 3. Only layer 6, which approximates to class 2, shows any variation from the predominance of class 1 folds produced by D2. However some layers for which T and t were not determined approximate to class 2.

Hence folds of D2 consisting mainly of convergent and parallel isogons with minor divergent isogons indicate that the folds probably result from the flattening of flexures initially induced by buckling and by similar folding of slip or flow type.

Fold stack and fold train inflection surfaces indicate that TIS is perpendicular to AS and SIS varies from being parallel to AS up to an angle of 80°, from the AS and hence approximate to class 1 and 2 folds. Values of Z/L (Table 6) are relatively constant for surfaces within one stack but vary between folds.

D2 folds in the Rampsbeck Schists differ in style to those described above from the Girrakool Beds and equate more closely with class 2 folds, possibly due to the movement parallel to S_2 and transposition of S_1 into S_2. Folds typical of D_2 from the Rampsbeck Schists are illustrated in Fig. 45 A to D. The folds are symmetrical unless transposition has occurred and are tight with an interlimb angle ranging from about 10° to 80° and hinge zones are relatively sharp with limbs being planar. The folds are much smaller than those recorded from the lower grade rocks, the largest folds observed having an amplitude of about 50 cm.

Apart from the D2 folds outlined above kink bands and chevron folds were observed in the Girrakool Beds. Bedding is kinked (Plate 12C) and both kink bands and the chevron folds were observed in S_1 (Plates 12, 13) indicating that they were formed later than S_1. Orientations of these folds indicate they were formed during the D2 phase.

The formulae derived in Chapter 1 (pp. 10-14) were applied to two chevron folds from Boundary Creek (GR 5002 2478) and the following results obtained:

Fold	θ	λ/L	A/L	V	A/λ
C1	84°	0.66	0.14	34%	0.21
C2	64°	0.53	0.41	47%	0.77

PLATE 13

A. Hand specimen slab of chevron fold in slaty cleavage with hinge zone changing from angular to rounded upwards in the stack for the antiform on the left hand side of the photograph. Minor quartz veining infills openings in the hinge region. Magnification x 1.

B. Tight chevron folds in highly cleaved mudstone with minor quartz veining emplaced in the hinge regions. Magnification x 1.

C,D. Outcrop scale mesoscopic chevron folds in highly cleaved mudstones. Pencil in Plate 13D is 0.14m long.

E. Interbedded siltstone and mudstone showing refraction of the cleavage through the siltstone layer and opening up of tension gashes which were subsequently filled with quartz. The black line indicates the path of one continuous cleavage plane trace through the specimen. Specimen from banks of Rockvale Creek (GR 4968 2419), magnification x 1.

Plates 13A to D were all taken from the same locality as Plates 12C to F.


A
B


C


D

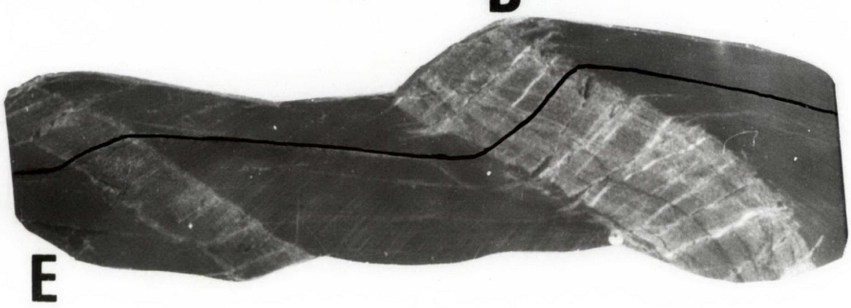
E

These are similar to other D2 folds and when plotted on the graphs of λ/L and A/L versus θ (Fig. 47) fall in a similar field.

Thirty-one kink bands from Boundary Creek west of the Rockvale - Aberfoyle road were measured to determine values of α, β and γ (terminology after Anderson 1968). The kinks vary from sharply angular kinks to slightly rounded ones and in most cases the distance between the two parallel surfaces (kink planes) was less than 2 cm although much larger varieties were recorded. The following observations were recorded in the field:

(1) sense of displacement of the foliation across the kink band (dextral or sinistral),

(2) orientation of the unrotated foliation outside the kink plane,

(3) orientation of the rotated foliation within the band,

(4) orientation of the kink planes.

Using an equal angle stereographic projection the following angles were determined:

(a) α - angle between the unrotated foliation and kink plane,

(b) β - angle between the rotated foliation and kink plane,

(c) γ - angle between rotated and unrotated foliations.

Of the 31 kink bands measured 14 display a dextral sense of rotation and 17 are sinistral. Mean values for α and β for dextral and sinistral kinks are presented below:

	α	β
Dextral	63.2°	84.1°
Sinistral	56.4°	82.0°
Both	59.5°	83.0°

For both dextral and sinstral kinks the mean values of α are around 60°. However the mean value for dextrals is considerably more than that for sinistrals. Anderson (1968) found the reverse situation for kink bands from Northern Ireland and concluded there was no obvious reason for the departure from symmetry.

For β, significantly higher mean values were recorded. Anderson (*op. cit.*) considered that β should not be smaller than α if the kink bands developed solely by slip on the foliation planes and the slip was confined to the layers between the kink planes. This condition was found to be satisfied in 26 out of the 31 examples (Fig. 49A) and 29 kinks fell within

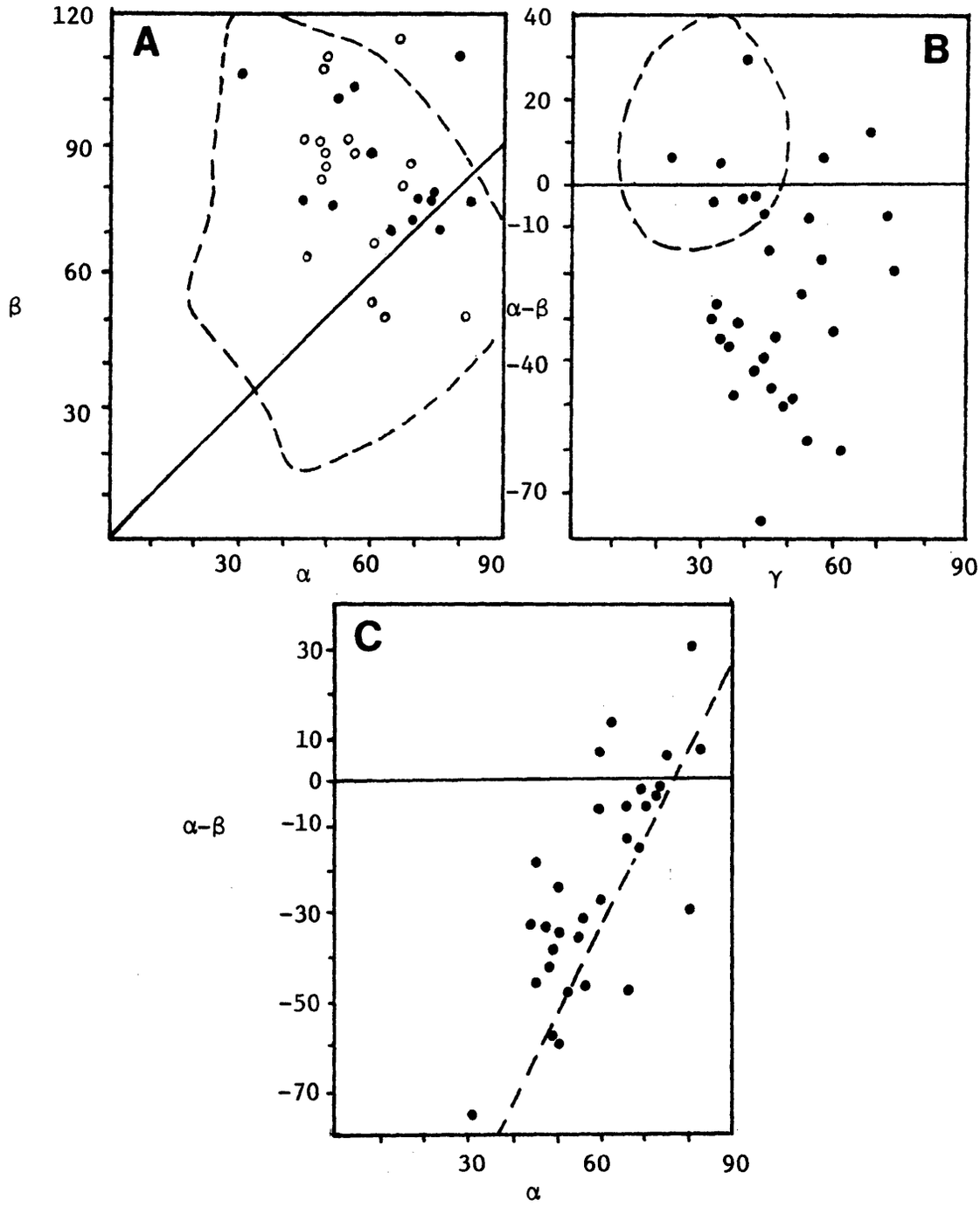

Fig. 49 A: Plot of β against α for each of 31 kink folds. Dashed field indicates limits of 513 kink bands plotted by Anderson (1968, Fig. 8). • - dextral kinks, ○ - sinistral kinks.

B: Angular deviation of kinked foliation (γ) compared with α-β. Dashed field is that of Fyson (1968, Fig. 3).

C: Angle between unrotated foliation and kink plane compared with α-β. Dashed line is average trend line of Fyson (1968, Fig. 4).

the field of Anderson's (*op. cit.*, Fig. 8) kinks. The opposite relationship was reported by Fyson (1968) from Nova Scotia where $\alpha > \beta$ in 65 out of 94 sinistral kinks. Only 7 of the Boundary Creek kinks fall within the field of Fyson on a $\alpha - \beta$ versus χ diagram (Fig. 49B). The graph exhibits no obvious trends but the variation of $\alpha - \beta$ correlates with α (Fig. 49C). Here the kinks with highest α tend also to have the highest $\alpha - \beta$. These data correlate readily with the average trend line for the kinks described by Fyson (1968, Fig. 4).

From the above data it can be concluded that the kink bands formed by slip which was confined to the rotated foliation between the two kink planes.

D3 Mesoscopic Structures

There is no evidence of D3 structures from the Girrakool Beds, these only being present in the higher metamorphosed parts of the Rockvale Block.

PLANAR STRUCTURES

This is represented only by the axial surfaces of rare folds in S_2 and is not developed as a distinct foliation. Where observed S_3 appears to have a constant orientation approximately at 90° to S_2.

LINEAR STRUCTURES

The only linear structures associated with D3 which were observed were the axes of the minor folds in S_2 and no lineations resulting from intersection with So, S_1 or S_2 were found.

MESOSCOPIC FOLDS

These folds occur as broad gentle steeply plunging folds with large interlimb angles and are manifestations of gentle flexuring of S_2 and because of poor outcrop over much of the high grade Rampsbeck Schists are relatively rare in comparison with folds produced by D1 and D2.

Mesoscopic Faults, Joints, Quartz Veins

Numerous mesoscopic faults were observed in the Rockvale Block with both dextral and sinistral senses of displacement which ranged from about 1 mm to over 1 m and a detailed analysis of them have not been attempted. Korsch (1967) at the "Fossil Locality" (GR 4992 2395) recorded normal faults with 5 cm displacement and strike of 110/N/85 in bedding striking dominantly to about 025°, and similar faults with an orientation of 040/NW/60 in bedding with a strike of approximately 090° and concluded that these minor faults were early features formed prior to D2 and were subsequently deformed by the D2 deformation.

Abundant jointing occurs in all lithologies and no recognisable patterns were observed in small areas and random distributions occurred on stereographic projections from each macroscopic domain (see composite net Fig. 50A).

Numerous quartz veins occur and were found as infilled joints, as en echelon veins in coarse lithologies and as concentrations in the hinge areas of folds particularly those formed during D2. Random orientations of planar quartz veins from several domains were also observed (Fig. 50B).

MACROSCOPIC STRUCTURE OF THE ROCKVALE BLOCK

Introduction

The presence of macroscopic structures, including major folds, in the Rockvale Block has been inferred from changes in the orientation of the mesoscopic structures. Because of the monotonously uniform nature of the sequence it was not possible to use marker horizons to delineate any major structures. Hence techniques used for the macroscopic analysis are similar to those used for the Coffs Harbour Block (p.30ff). Idealised trend line maps for So and S_1 have been constructed (Maps 4, 5) and the macroscopic geometry has been studied on four scales. The resolution of results varies quite markedly on the different scales, as discussed at length below.

A. Localities studied in Detail (Mesoscopic Scale): Although outcrop over the whole region can be regarded as poor, there are some very good creek exposures about 100 m by 50 m in size and five of them were selected for detailed analysis, each being mapped at an initial scale of one inch to five feet, which was necessary to unravel the mesoscopic geometry.

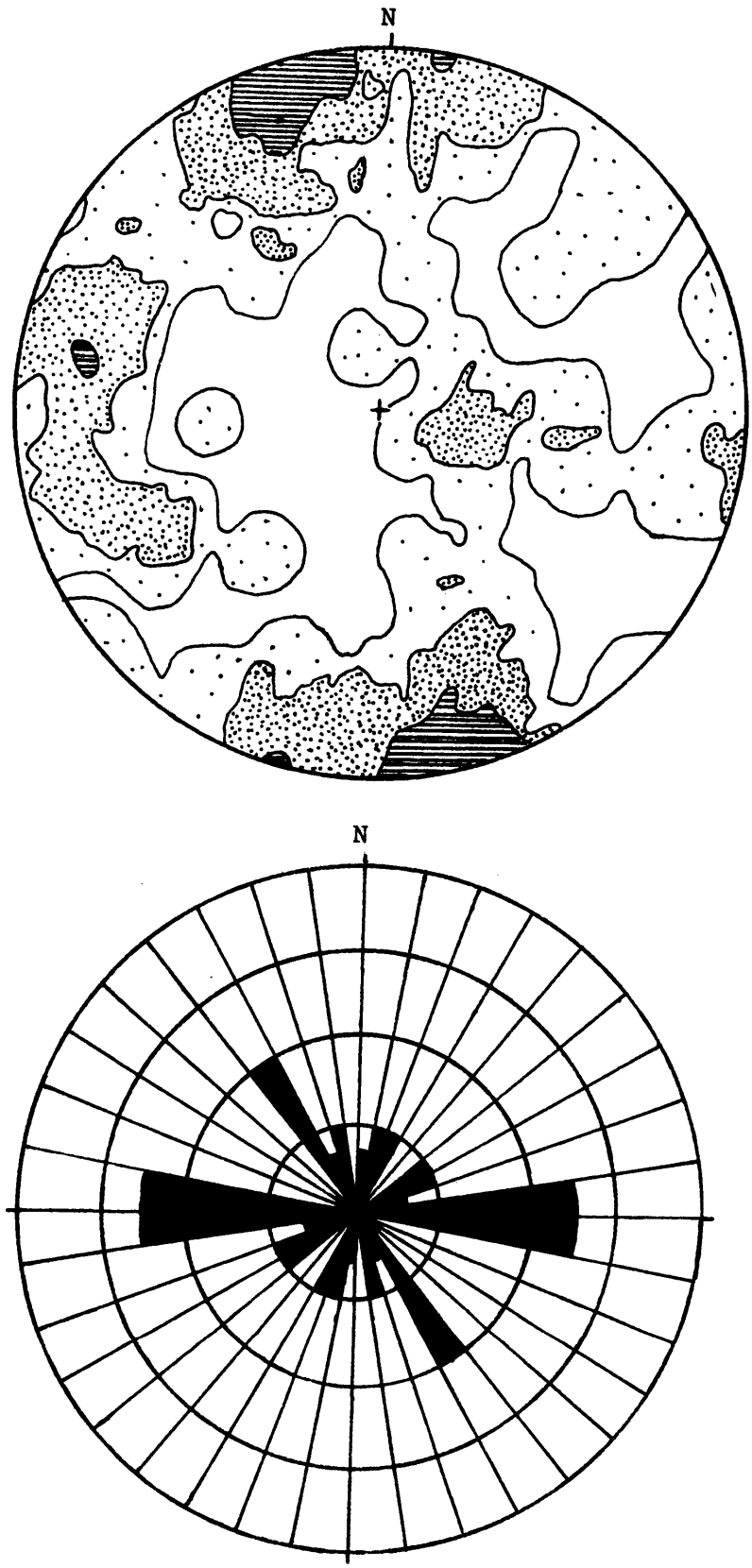

Fig. 50 A: π plot of 71 joints from Rockvale region. Contours 1-4-8% per 1% area.

B: Rose diagram for strikes of quartz veins from the Rockvale area. N = 27. Spacing for concentric circles is two readings.

B. Homogeneous Domains (Small Macroscopic Scale): These range from about 100 m^2 localities to about 5 km^2 and the most exhaustive work in the Rockvale Block was carried out at this scale. The Girrakool Beds around Rockvale have been divided into 13 domains based on orientation patterns of mesoscopic structures, as outlined on Map 3. The domains are usually one dimensional, that is, creek sections, the two dimenstional picture being difficult to determine because correlation between creeks is very difficult due to lack of marker horizons. Nevertheless it was possible with some suppositions to determine the geometry at this scale.

C. Medium Macroscopic Scale: This scale involves the whole area covered by the 13 domains at Rockvale and also other areas of similar scale (up to 100 km^2) within the Rockvale Block. Using maps of trends of form surfaces, and synoptic stereographic plots, it was possible to derive a clear picture of the macroscopic geometry at this scale for the Rockvale district, but not for the whole Block.

D. Large Macroscopic Scale: This covers the whole of the Rockvale Block (scale approximately 500 km^2) and it is possible to present only an approximation of the geometry at this scale.

Work on the four scales is discussed in turn below.

A. Localities Studied in Detail

1. "DOUBLE FOLD LOCALITY" (DFL)

This locality is much visited because of the complex structures in rocks that contain the Permian fossil *Atomodesma* sp. at the nearby "Fossil Locality". The DFL is at GR 4981 2405, measures about 113 m by 34 m, and consists of interbedded fine sandstones and mudstones which appear to have suffered two periods of deformation. Several undergraduate students of the Department of Geology, University of New England, have studied it for Third Year Projects (Harris 1963, Nott 1967, McClung 1968, Price 1969, Jeffery 1971, Pearcey 1974). Each report presents different results in part because of differences in sampling intensity and in part because of failure to recognise some structural elements. Hence the present writer completely remapped the locality and collected 1500 measurements of orientations of structural elements. Where appropriate a relevant undergraduate project is mentioned but the interpretation given here is the sole work of the present writer.

Figure 51 provides a detailed trend-line map of bedding planes at the DFL. Bedding is very well developed with the average thickness being 5-15 cm and the maximum about 30 cm. Not every bed is shown on Figure 51 but care has been taken to ensure that beds traceable over long distances are included. From this pattern it can be seen that the axial surface traces of the dominant folds trend NW-SE, and that those of the subordinate folds trend NE-SW.

Where possible, facing evidence was noted and indicates that all the bedding is overturned. Consequently all folds are either anticlinal synforms or synclinal antiforms. The dominant folding consists of a series of asymmetrical folds, the long limbs being the northern limbs of the synclinal antiforms. Due to lack of continuous outcrop, often in critical areas, it is not possible to trace individual beds over great distances and hence it is not possible to delineate the en echelon fold pattern inferred by Harris (1963) or the three sets of en echelon folds suggested by Jeffery (1971). Nevertheless the observed pattern is similar to a cross-section through a pattern of en echelon folding illustrated by Campbell (1958, Fig.5) where the asymmetrical folds have two short limbs separated by an extremely long limb.

The styles of folds are illustrated in Plate 11. The three D1 folds analysed previously (pp. 58-59) were all collected from this locality. The analysis of them show that the dominant folds have a complex geometry but that those in the competent layers may be equated with parallel folds modified by flattening. The folds are observed to change their shapes up and down the stack, but no decollements are seen and it is possible to trace one synclinal antiform for a distance of over 22 metres along the axial surface trace.

A summary of the orientation of the structural elements is presented in Table 7, along with the orientation of the kinematic axes for the second period of folding. The great circle for bedding suggests deformation by an episode of plane cylindrical folding. Cleavage is not readily observable at this locality because the flow of muddy material into hinge zones between the more competent sandy layers has tended to inhibit the development of cleavage planes. Groove casts (Lo) define a partial great circle, and assuming that they were initially parallel, have acted as passive lineations being redistributed along a great circle by a period of folding.

Plots of measurements of 107 interlimb angles (Fig. 53B) show a

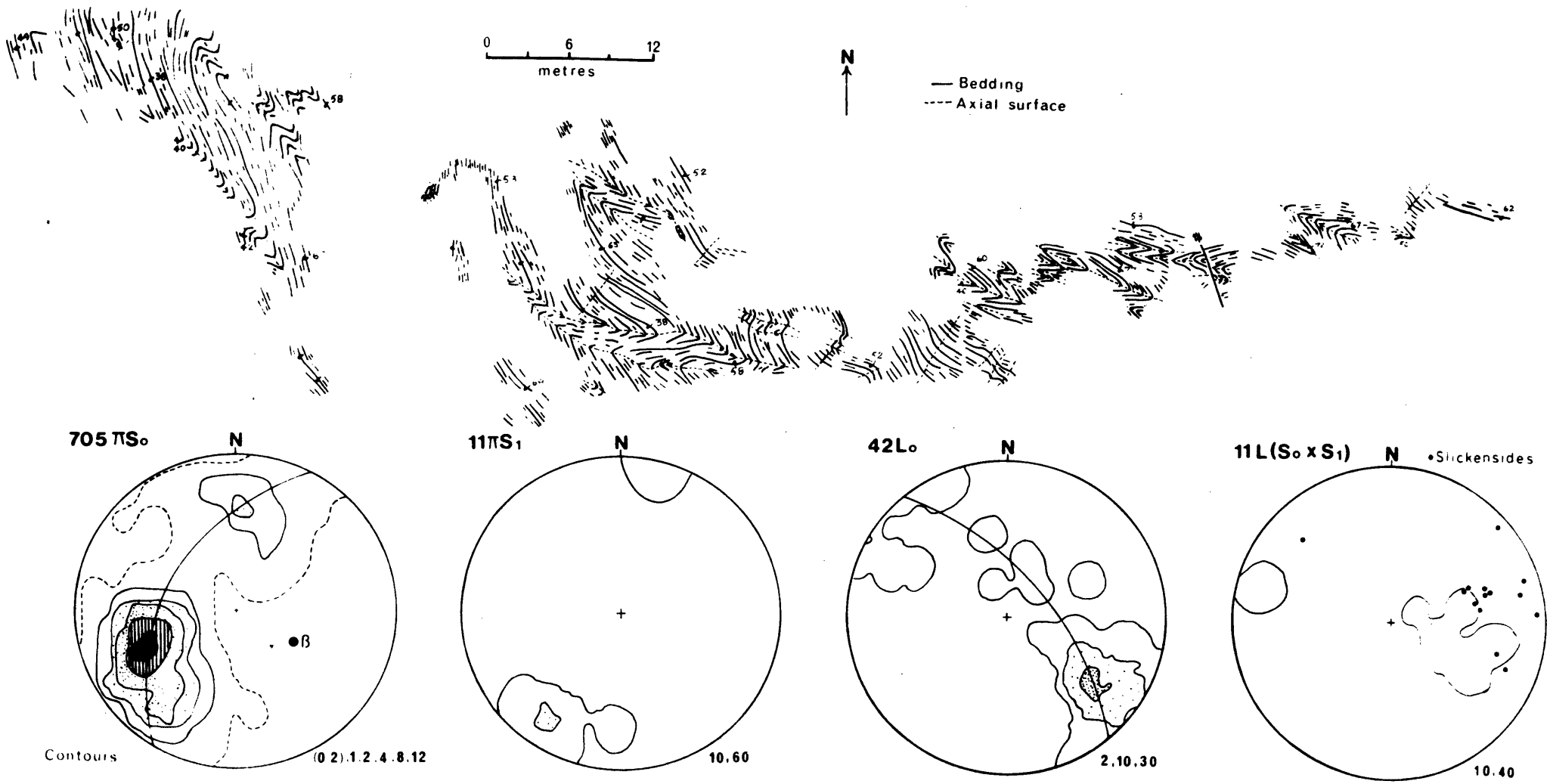

Fig. 51: Structural map and stereographic projections for the Double Fold Locality at Rockvale.

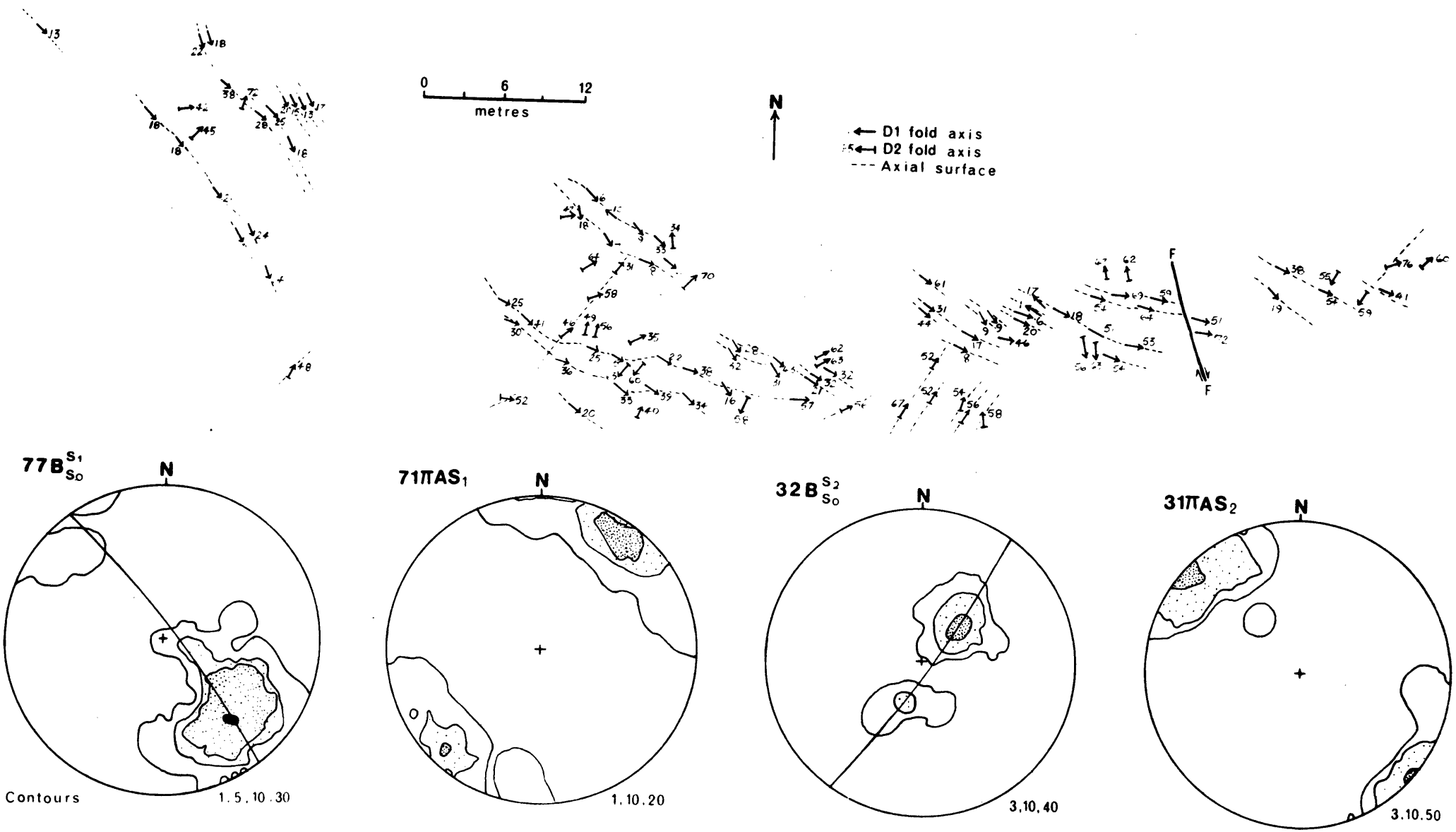

Fig. 52: Stereographic projections and map of fold axes for mesoscopic folds from the Double Fold Locality.

DOUBLE FOLD LOCALITY

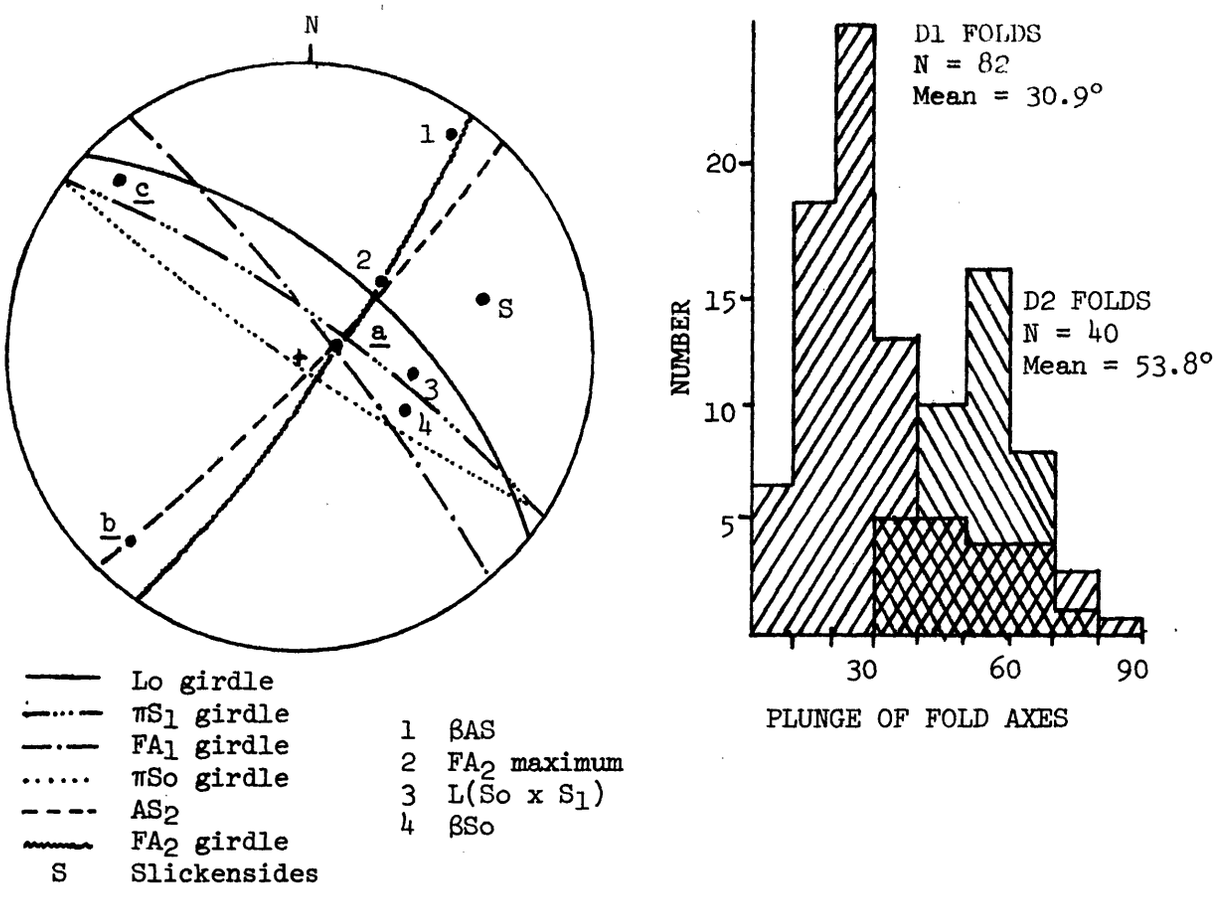

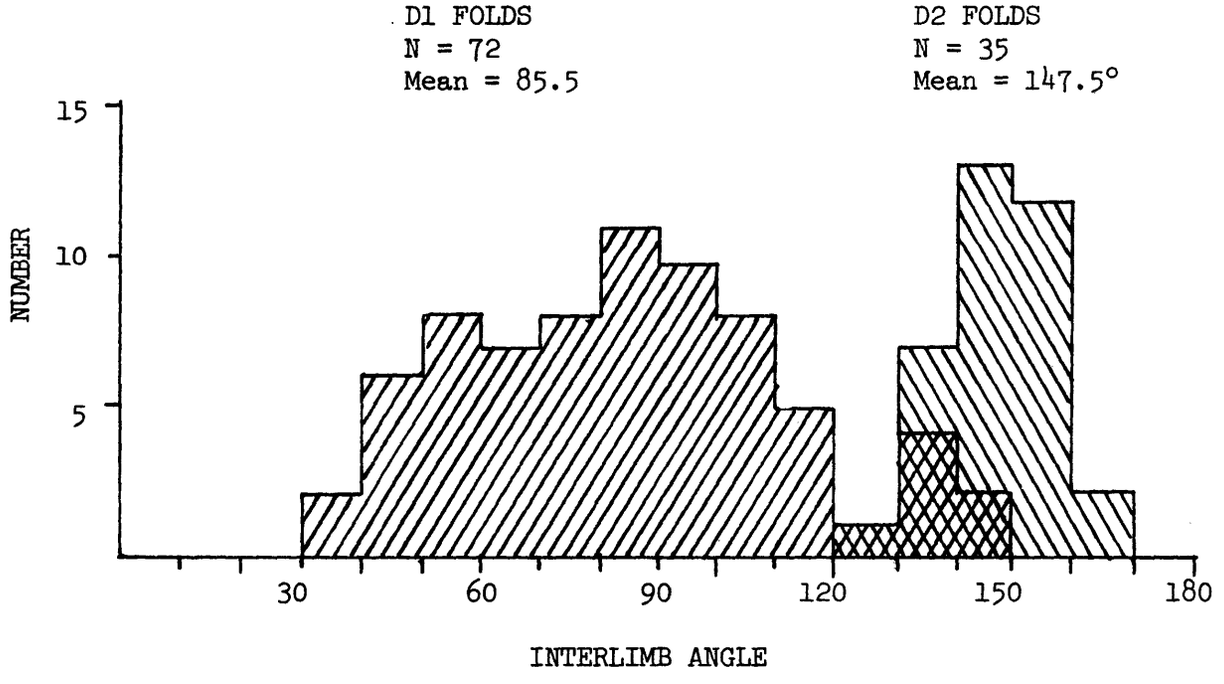

Fig. 53: Histograms and synoptic stereographic projection for the Double Fold Locality.

Table 7: Summary of geometry of structural elements plotted on stereographic projections for the detailed localities, Rockvale area

Domain	πSo	Lo	πS_1	L(So x S_1)	$B^{S_1}_{So}$	πAS(So x S_1)	$B^{S_2}_{So}$	πAS(So x S_2)	Kinematic axes
Double Fold Locality	great circle 030/W/44 β=46 to 120	partial great circle 140/NE/60	point maxima 11 to 215-plane 125/N/79	point maxima 52 to 104	partial great circle 142/N/80	elongated point maxima or partial great circle	partial great circle 035/E/80	elongated point maxima 8 to 313 plane 043/E/82	a = 79 to 090 b = 8 to 221 c = 10 to 313
Lock Creek Locality	partial great circle 150/SE/35 β=55 to 060	-	-	-	plunge moderately to S and SE	partial great circle 063/ NW/36 β=54 to 153	point maxima 55 to 047	indistinct point maxima 11 to 320 plane 050/E/79	-
Balaclava Stream Locality	indistinct picture - two girdles?	-	-	-	partial great circle girdle 155/E/75	elongated point maxima 28 to 249 159/E/62	subvertical plunge	strike NE-SW, steep dip to SE	a = 70 to 113 b = 11 to 233 c = 17 to 326
Boundary Creek Locality	great circle girdle β=42 to 095	-	-	-	-	-	point maxima 46 to 078	point maxima 4 to 164 plane 074/N/86	-
Fossil Locality	divided into four subdomains	-	-	-	-	-	point maxima 40 to 074	average plane 060/N/85	-

bimodal distribution with maxima of 86° and 147°, and these can be related to the two periods of folding observed at this locality. D1 mesoscopic folds have interlimb angles ranging from 30° to 150° and fold axes have changing plunges along a single axial surface trace (Fig. 52). D2 mesoscopic folds have interlimb angles ranging from 120° to 170° and as all folds are in bedding, they are B^{S2}_{So} folds. B^{S2}_{S1} folds were not observed at this locality.

The DFL has been affected by two periods of folding. The first period produced folds plunging dominantly to the south-east with an almost vertical axial surface, and varying in tightness from open to almost isoclinal. As observed on the synoptic diagram (Fig. 53A) the β_{So}-points produced by the πSo girdle and L(So x S_1) maximum are almost coincident, and possibly define the approximate position of the D1 fold axis. Nevertheless the B^{S1}_{So} axes define a partial great circle. The groove casts also fall on a partial great circle, reflecting the second period of deformation and not the first. This rare occurrence is readily explained by the fact that most of the beds are facing to the west and dipping to the east, and all groove casts were observed on the limbs of the D1 folds, which reflect the later D2 folding.

In conclusion the D1 folds have a NW-SE axial surface with plunges ranging from subhorizontal to almost vertical (mean 31°). The D2 folds are more gentle and have a NE-SW axial surface with fold axes (B^{S2}_{So}) ranging from 30° to 80° with a mean of 54°. Using the method of Turner and Weiss (1963, p.486) the kinematic axes were determined using the intersection of the S_2 plane and the B^{S1}_{So} great circle. This also indicates deformation by the slip (or flow) mechanism.

Harris (1963) concluded that the pattern of folding at the DFL is the result of drag of the bedding during discrete movements along a fault plane of orientation 164/E/50 located adjacent to the outcrop. Price (1969) considered that the two mesoscopic fold periods are in face one period of deformation which was produced by gravity sliding hypothesis and then externally rotated to its present position. Jeffery (1971) postulated that the folds formed as a consequence of dextral movement along a N-S shear zone located about 400 m east of the DFL.

No evidence of the inferred faults of Harris and Jeffery was found and it is considered that it is premature to attempt an interpretation of the folding mechanisms until the picture at the larger scales has been

examined. Folds of a similar style and orientation to those at the DFL occur at many localities on the Rockvale area and a complex fault pattern would be required if the interpretations of Harris or Jeffery were found to be correct. The interpretation of Price (*op. cit.*) can only be confirmed or denied after the regional picture has been examined.

2. LOCK CREEK LOCALITY (GR 4954 2397)

This area of almost continuous outcrop 37 m x 22 m on the bank of Lock Creek consists of a series of mesoscopic folds similar in style and intensity to those at the DFL. The area is cut by numerous mesoscopic faults, usually traceable only over 3 metres. One large shear zone over 12 m long and up to 0.3 m wide contains slivers of bedded sediments.

A very weathered acid dyke 0.7 m wide striking 058° cuts across the bedding. It contains a well developed foliation, possibly a set of cooling joints, of orientation 010/E/52.

The outcrop in Lock Creek is unusual in that it is one of the few localities in the Rockvale area where there is a significant amount of upright facing evidence. The only overturned beds recorded here are on a limb of a tight mesoscopic fold in the western portion of the locality (Fig. 54).

A graph of interlimb angles (Fig. 55A) exhibits a bimodal distribution with means at 45.1° and 132.8°. Values range from 27° to 164° and the bimodal distribution can be equated with D1 and D2 folds respectively. D1 fold axes have a mean plunge of 37.4° and D2 of 54.7°.

A summary of the orientation of the structural elements is given in Table 7. Poles to bedding define a partial great circle which is indicative of cylindrical folding. Cleavage is not developed to any marked extent, possibly because pelitic rocks are rare.

The folds of the first period of deformation are tight (or closed), plunge moderately to the south or south-east and have axial surfaces plotting in two point maxima. The scattered distribution of these elements probably results from subsequent deformation by D2.

D2 consists of gentle folds plunging steeply to the north-east and having axial surfaces trending northeast-southwest. The β-pole to the So girdle also lies in this plane indicating that the girdle is a result mainly of D2. Minor deflections of data away from the girdle might represent the limbs of tight D1 folds. All beds dip to the east even though some are upright and others overturned. The β-point defined by the spread of AS1

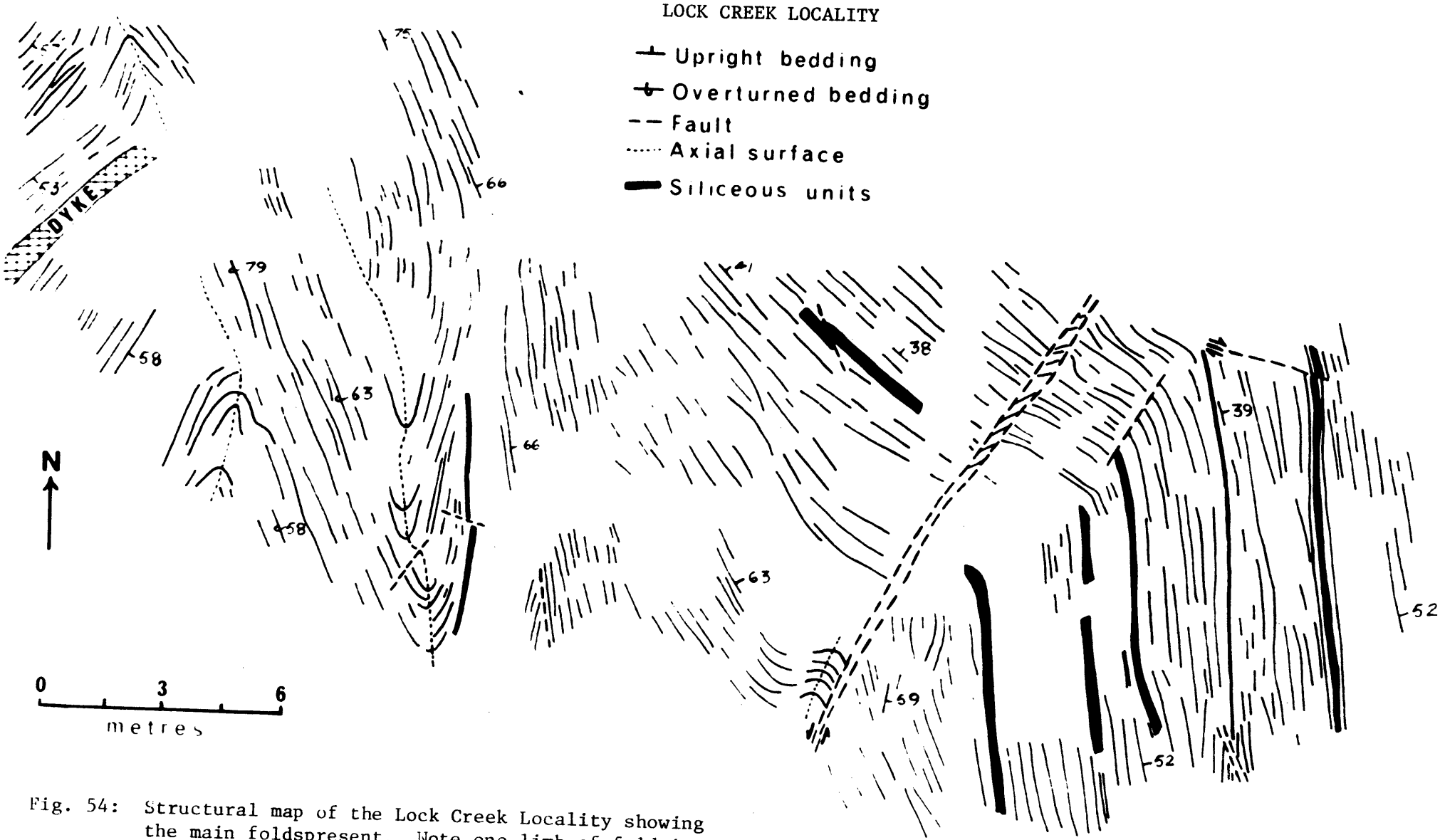

Fig. 54: Structural map of the Lock Creek Locality showing the main foldspresent. Note one limb of fold is overturned whereas the other limbs are right-way-up.

LOCK CREEK LOCALITY

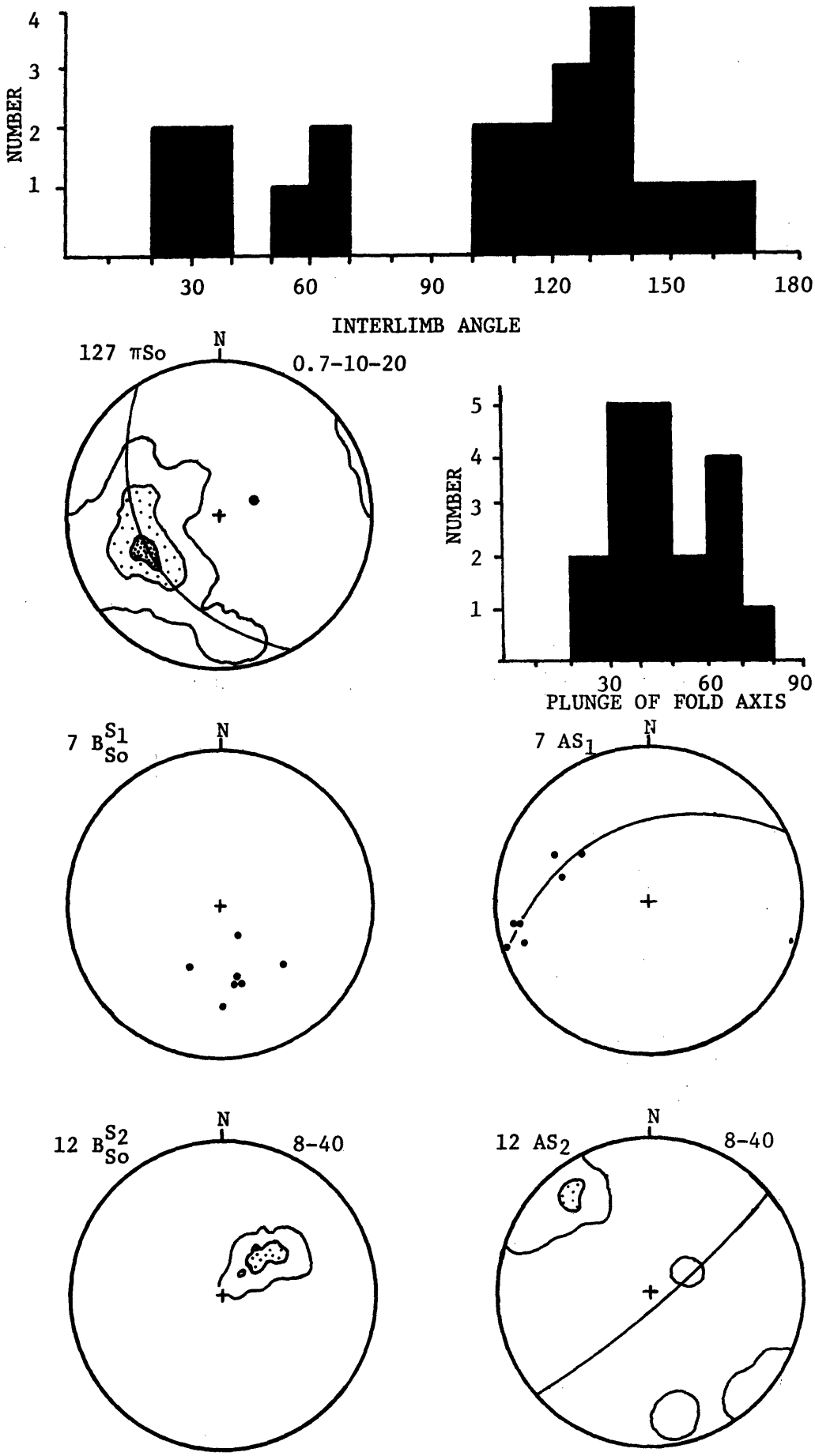

Fig. 55: Histograms and stereographic projections for the Lock Creek Locality.

falls close to AS2 indicating that it is the fold axis ($B_{S_1}^{S_2}$) for the second period of folding. The $B_{So}^{S_2}$ net probably represents a biased sample as these data would be expected to fall along a girdle because So was non-planar prior to the second deformation. In most respects the geometry of the Lock Creek Locality is very similar to that at the DFL.

3. BALACLAVA STREAM LOCALITY (GR 4954 2390)

This locality of almost continuous outcrop over an area 24 m x 6 m on the bank of Balaclava Stream has been affected by two periods of folding (Fig. 56) similar to those at the DFL and Lock Creek localities. There are three mesoscopic faults, traceable only over about 3 m, and drag on one of them appears to have affected one D2 fold. Displacement appears to have been less than 30 cm in all cases. Facing evidence indicates that all bedding is overturned.

Interlimb angles (Fig. 57) range from 25° to 145°. D1 folds have a mean of 77.1° whereas D2 folds have a mean of 139.7°. Plunges for fold axes (Fig. 57C) range from 19° to 88°. D1 folds have a mean of 41.3° and D2 folds have a mean of 78.7°. Consequently interlimb angles and plunges of fold axes can be used to distinguish between D1 and D2 folds.

The D1 and D2 folds exhibit similar patterns to those observed at the DFL. The ΠSo plot appears confused because of the folding of a planar surface by D1 and subsequent deformation of the resultant nonplanar form surface by D2 to produce the present picture. To achieve a clear picture this domain should be broken into several subdomains. Assuming an average orientation of D2 axial surfaces of 056/SE/73 then the intersection with the plane defined by $B_{So}^{S_1}$ can be used to locate the kinematic axes. The movement picture will be discussed later.

4. BOUNDARY CREEK LOCALITY (GR 5030 2465)

This locality of size 15 m x 12 m consists of well bedded overturned sediments deformed to produce the fold pattern illustrated in Figure 58. Facing evidence indicates that all bedding at this locality is overturned. A dextral fault with drag of the beds and a displacement of approximately 5 m intersects this locality and has possibly affected some folds.

The ΠSo plot (Fig. 59B) exhibits a distinct great circle, and the fold axes (Fig. 59D) form a point maximum, suggesting that there has been only one deformation which produced cylindrical folding. Plunges of fold

BALACLAVA STREAM LOCALITY

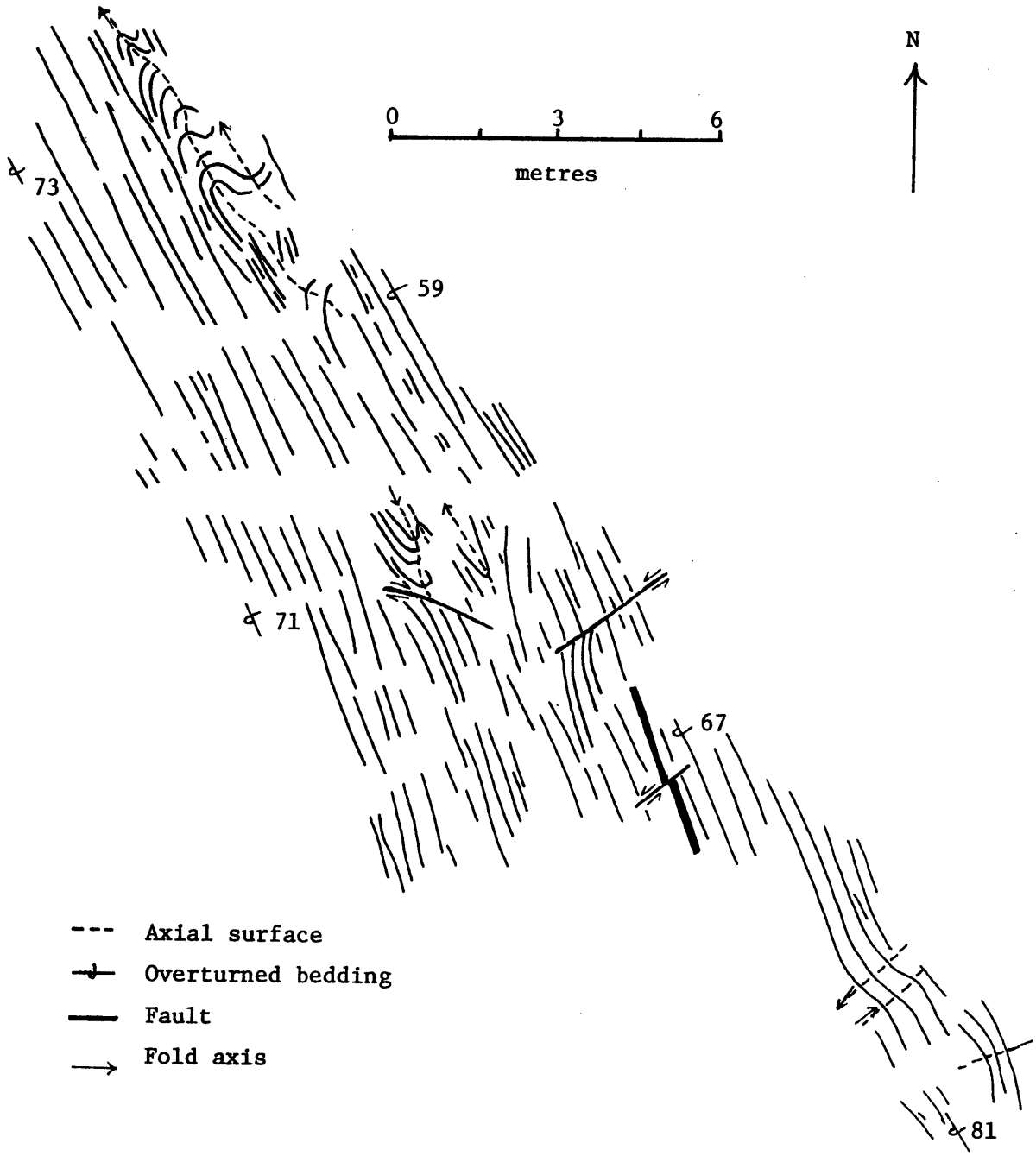

Fig. 56: Strike line map of bedding showing two periods of mesoscopic folding at the Balaclava Stream Locality.

BALACLAVA STREAM LOCALITY

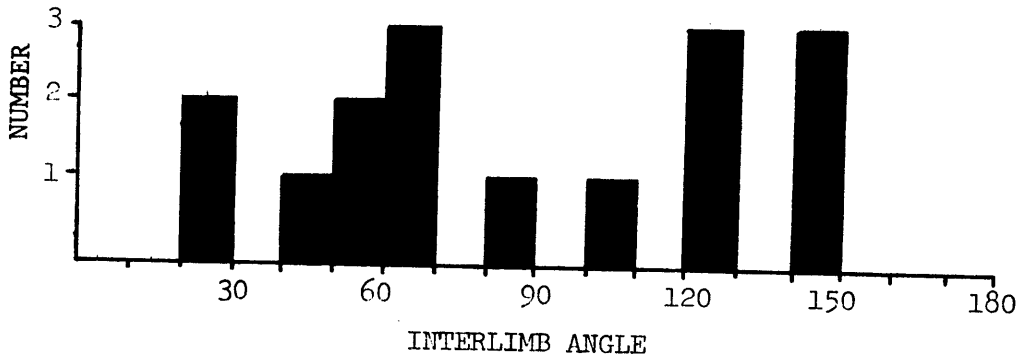

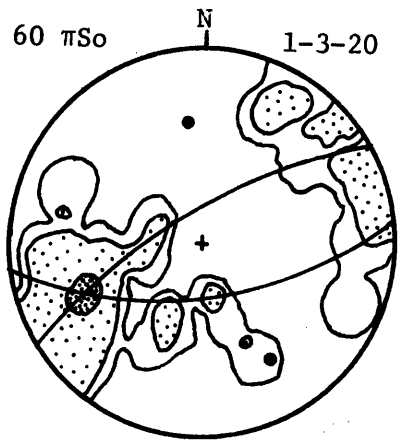

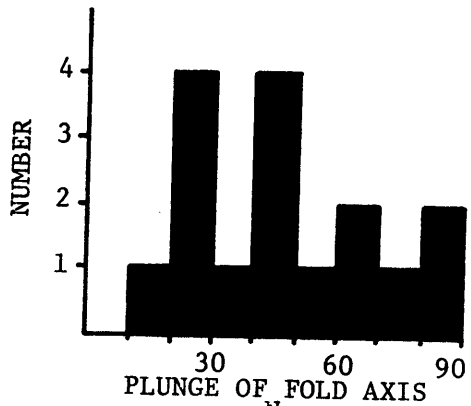

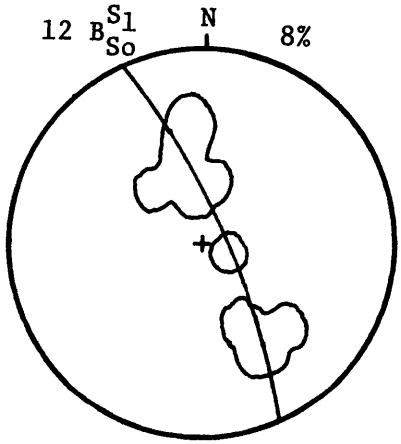

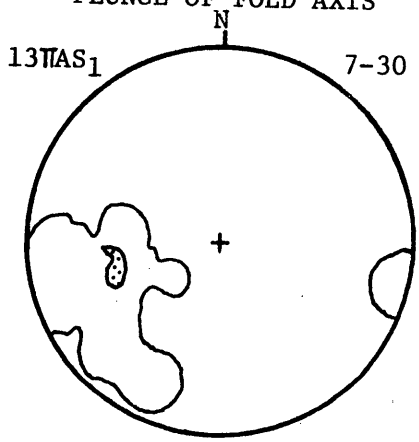

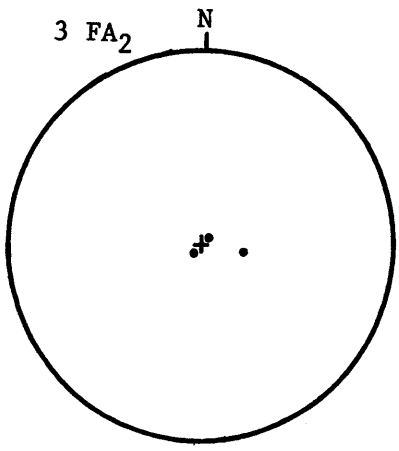

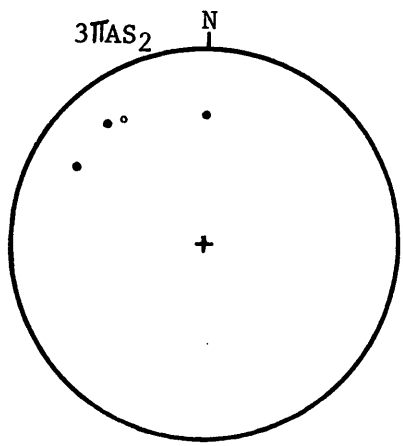

Fig. 57: Histograms and stereographic projections for the Balaclava Stream Locality.

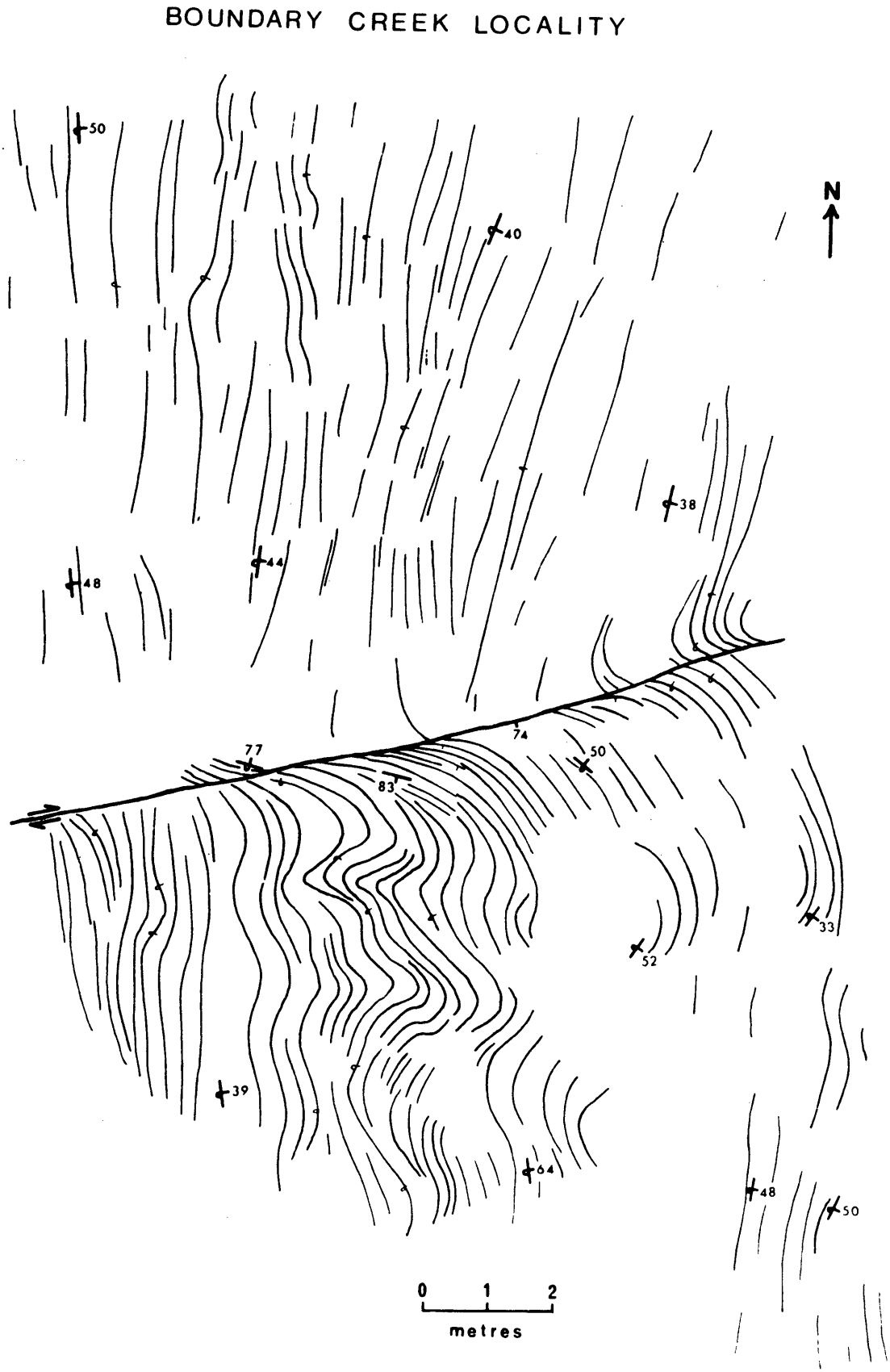

Fig. 58: Structural map for the Boundary Creek Locality. Note majority of beds apart from some close to the fault are overturned.

BOUNDARY CREEK LOCALITY

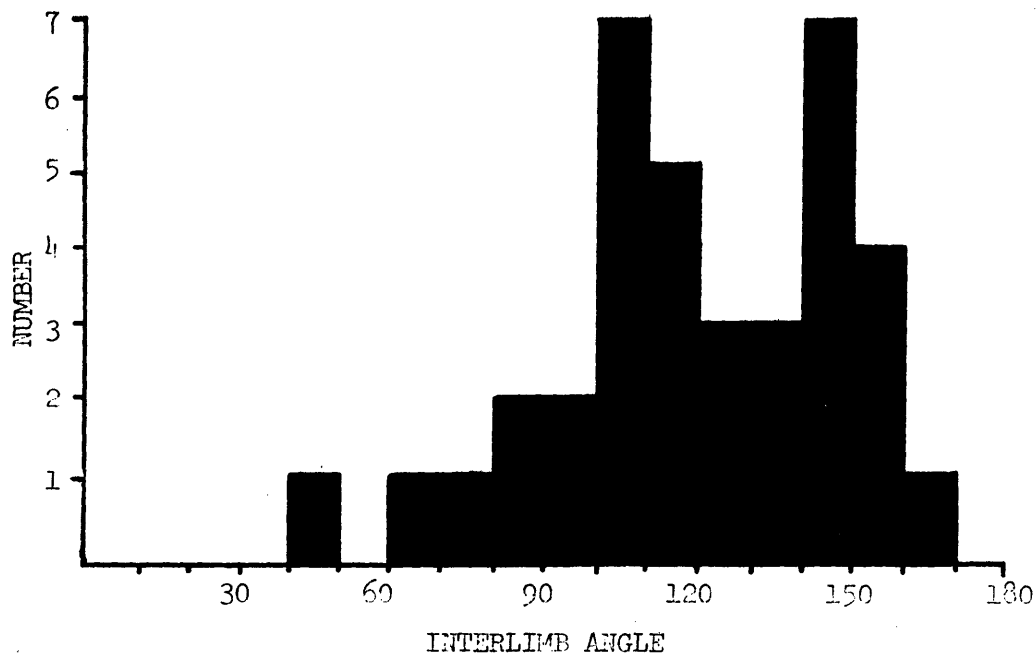

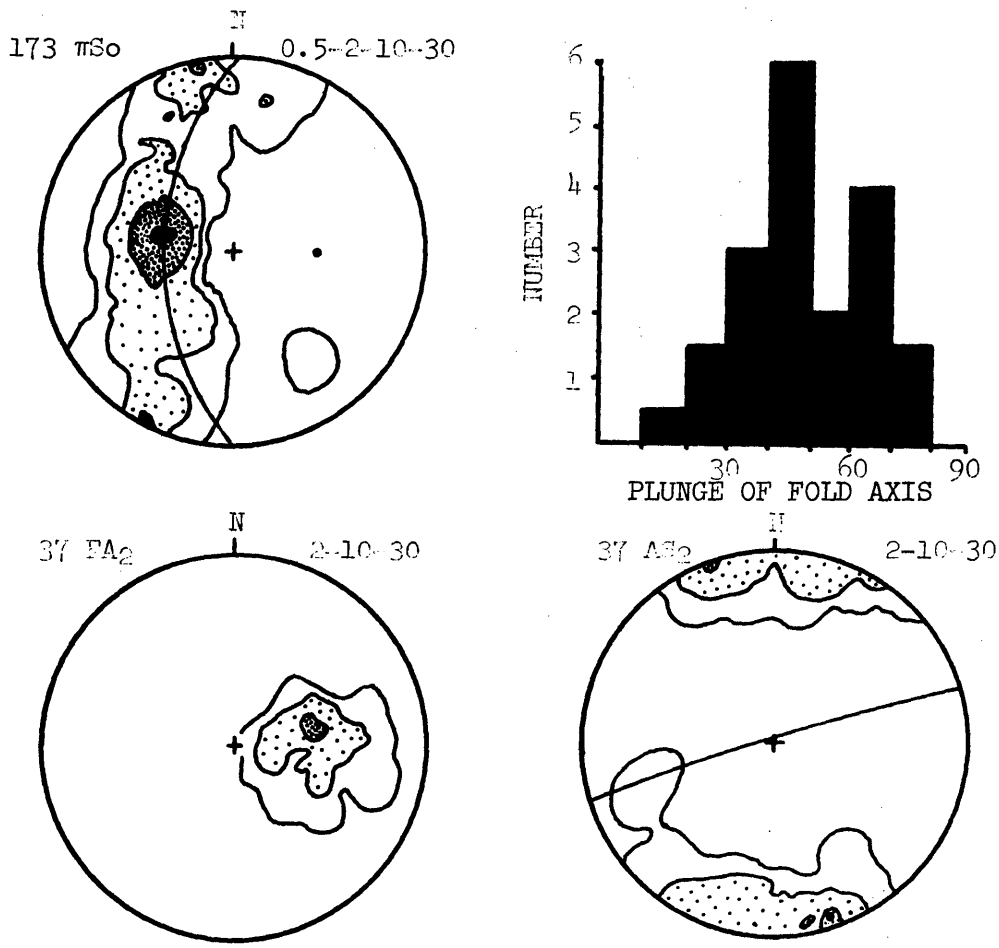

Fig. 59: Histograms and stereographic projections for the Boundary Creek Locality.

axes range from 18° to 77° with a mean of 48.9° (Fig. B).

A problem is to decide which deformation formed the folds. The interlimb angles range from 46° to 158° with a mean of 120.0° and hence could belong to either D1 or D2. The style of folds has been shown to be unreliable as a guide to identifying different deformational episodes (Park 1969, Williams 1970), but the orientation of the structures can be used.

If the folds are the products of D1 then subsequent deformation by D2 has not occurred or has been so slight so that the effects are not noticeable. On the other hand if the folds resulted from D2 then D1 must have been on a macroscopic scale larger than the sacle of this locality because So must have been planar prior to D2 and hence the locality would have to be located on the limb of a macroscopic fold.

Because the fold axes and axial surfaces have average trends slightly north of east this locality is tentatively correlated with other products of D2 deformation. If this is correct $B^{S_2}_{S_0}$ fold axes plunging to the southwest would not be expected at this locality because only one limb of the D1 fold is present.

5. "FOSSIL LOCALITY" (GR 4992 2395)

The "Fossil Locality" (Fig. 60) consists of a series of well bedded sediments contining rare broken fragments of *Atomodesma* sp. indicative of a Permian age. In places chaotic bedding and slumping occurs and all bedding is overturned except in one portion of the locality. Permian rocks that seem to have been overturned and then folded more than once have attracted a lot of attention from visitors. Using the computer programs described in Appendix II, the area has been divided into four homoaxial domains each with a partial great circle defining β-points plunging shallowly to the east or northeast.

Domain	Girdle	β
I	140/SW/60	30 to 050
II	154/SW/63	27 to 064
III	170/W/54	36 to 080
IV	180/W/80	10 to 090

The picture in fact seems to be simple despite its complex appearance. Bedding has been deformed by one period of mesoscopic folding, producing folds larger than those at other localities and having fold axes trending northeast. This orientation is the same as D2 folds

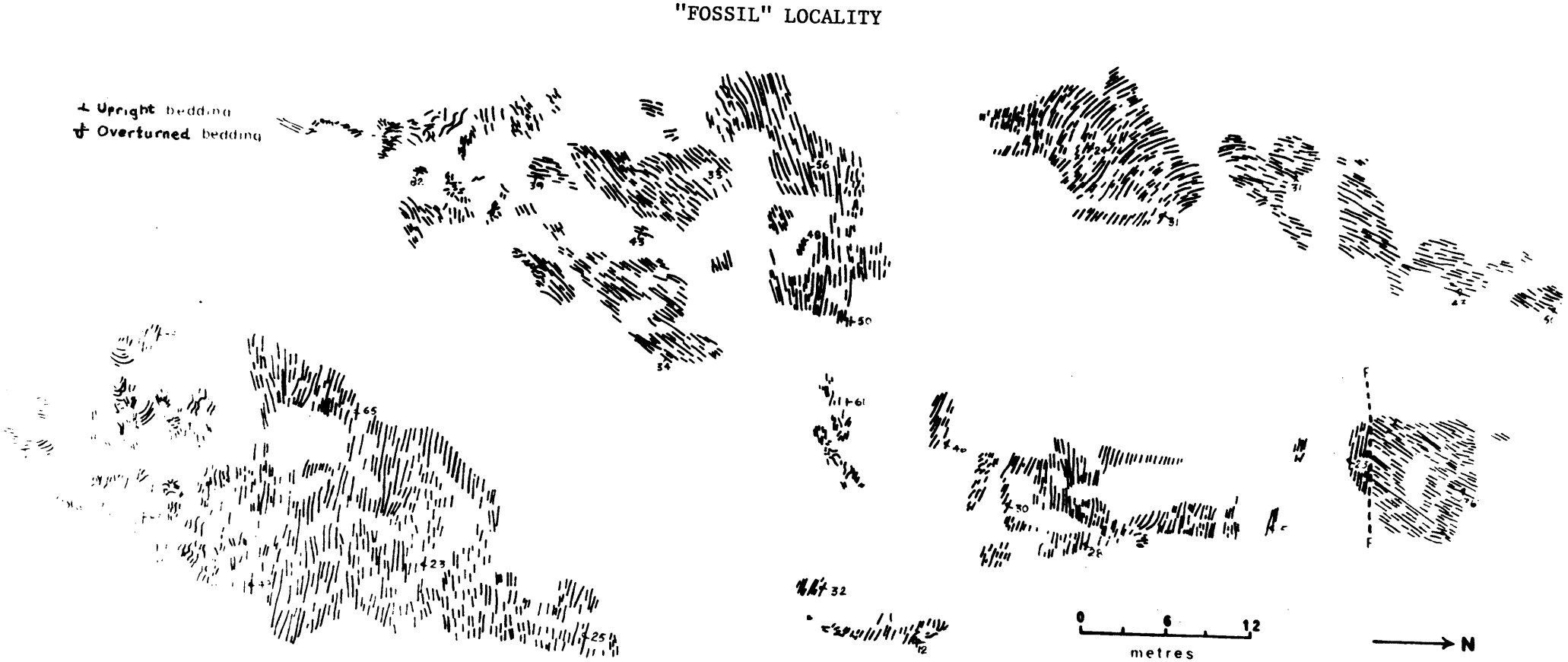

Fig. 60: Structural map showing main folds at the Fossil Locality. Note some beds are overturned while others are upright.

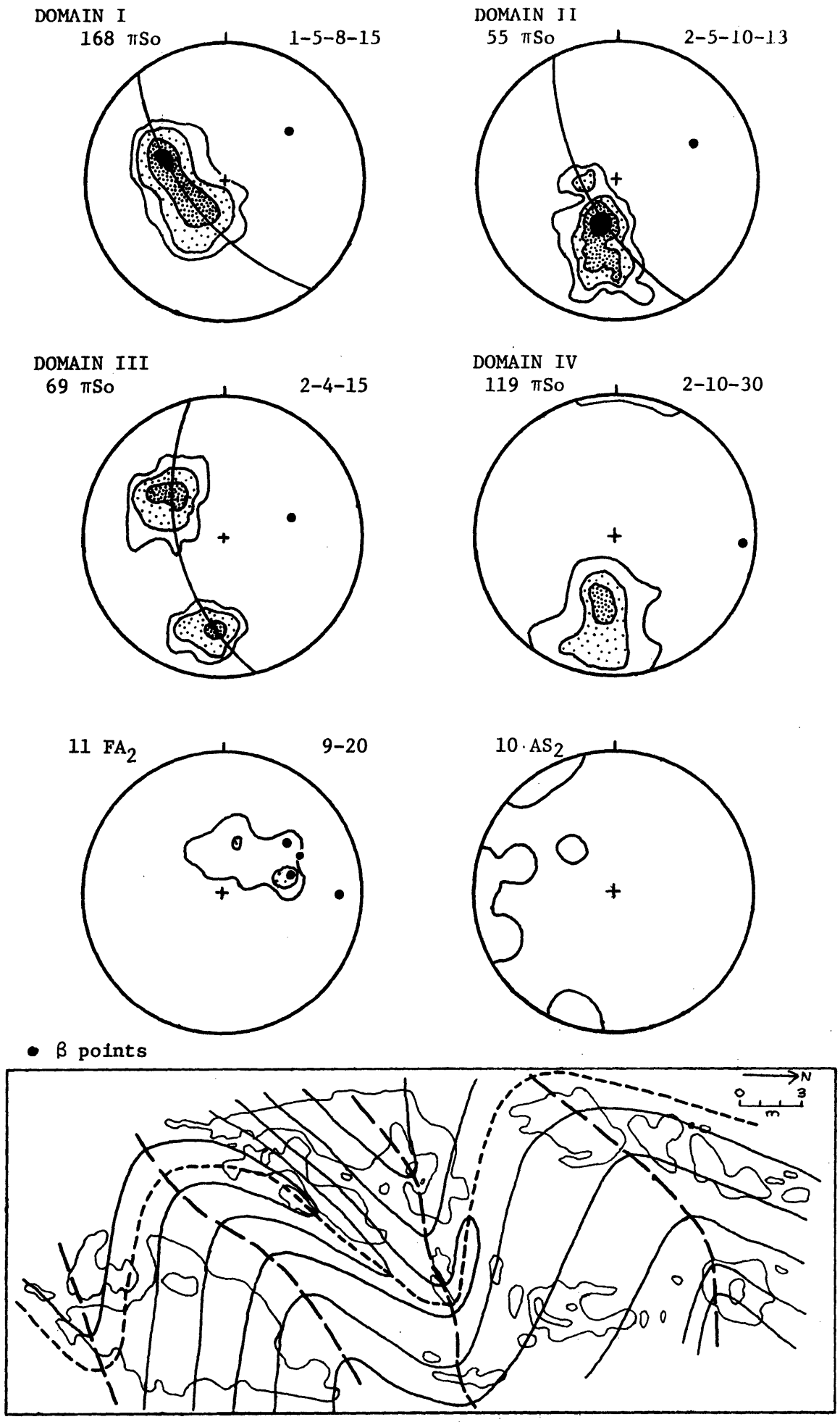

Fig. 61: Interpretation of fold pattern at the Fossil Locality.

described from the DFL. One problem is to explain the area of upright bedding. The most reasonable explanation is that there is a macroscopic nearly isoclinal syncline with an overturned eastern limb, and an axial surface striking approximately NNW.-SSE. and dipping steeply to the east. An interpretation of the structure is given in Fig. 61.

CONCLUSIONS DRAWN FROM THE DETAILED LOCALITIES

1. The Girrakool Beds of the Rockvale Block has suffered at least two periods of mesoscopic deformation.
2. The first episode (D1) produced folds varying from gentle to almost isoclinal and ranging in size from 0.3 m to larger than the scale of the outcrop. The axial surfaces of these folds were originally oriented approximately NW.-SE. with variations between N.-S. and E.-W., and were subvertical. Plunges were generally towards the southeast although some north-west plunges have been observed. In places these folds have been affected by the second period of deformation.
3. The second episode of deformation (D2) produced mesoscopic folds which vary from very gentle warps on the limbs of D1 folds to tight folds. D2 folds have axial surfaces trending NE.-SW. with almost vertical dips but there are some deviations and planes occur with strikes between N.-S. and E.-W. Fold axes plunge to both the NE. and SW. and are usually steep. The axes plunging NE. are predominant over the SW. ones because the NE. dipping limbs of D1 folds were longer than those dipping SW.
4. Except at two localities, both limbs of the D1 folds are overturned, and hence neither the D1 period of folding nor D2 appears to have caused the overturning. Because overturned beds occupy such a large area surrounding Rockvale (at least 100 km^2) a regional-scale mechanism must be sought to explain this phenomenon, as discussed later.

B. Homogeneous Domains (Domains 25-37)

Structural elements in these domains have been plotted on stereographic projections using program WULFF (Fig. II in Map Folder) and a summary of the geometry of the nets is presented in Table 8. The location of the domains are outlined on Map 3.

Table 8: Summary of geometry of elements presented on stereographic projections (in map folder) for macroscopic domains 25 - 40 from the Rockvale Block

Domain	So	Lo	πS_1	L(So x S_1)	$B^{S_1}_{So}$	πAS(So x S_1)	$B^{S_2}_{So}$, $B^{S_2}_{S_1}$	πAS(So x S_2, S_1 x S_2)	B for kinks	πAS for kinks	Kinematic axes
25	great circle at 096/S/50 β = 40 to 006	three points, average 4 to 172	partial great circle 100/N/10 β = 80 to 190	scatter with point maxima at 87 to 090	-	-	four readings average 35 to 006	four readings, average 025/W/80	-	-	-
26	partial great circle 077/S/10 β = 80 to 347	-	two points, average 129/NE/77	one point 80 to 032	two points, average 64 to 320	two points, average 153/E/76	-	-	one reading from dextral kink 70 to 018	two readings average 015/E/75	-
27	partial great circle 002/W/20 β = 70 to 092	-	point maxima at 4 to 357 defines plane 087/S/86	point maxima 68 to 115	point maxima 64 to 126	strike NW-SE sub-vertical dip	-	-	one reading from dextral kink 75 to 096	two readings average 031/SE/76	
28	great circle girdle 128/S/25 β = 65 to 038	scatter due to initial non-parallelism	partial great circle 140/SW/25 β = 65 to 050	great circle girdle 127/N/58	-	-	point maxima 61 to 036	point maxima at 20 to 142 defines plane 052/W/70	-	-	a = 57 to 020 b = 26 to 242 c = 20 to 142
29	partial great circle 096/S/50 β = 40 to 356	-	partial great circle 140/SW/20 β = 70 to 050	point maxima 50 to 090	two points NW-SE trend variable plunge	two points define plane 120/S/86	average point maxima at 50 to 010	five points, average plane about 010/vert	dextral kink plunge to NW, sinistral plunge to SE	both types strike SE-NW, opposite dip	a = 75 to 175 b = 14 to 014 c = 3 to 283
30	great circle 016/W/30 β = 60 to 106	great circle 150/NE/60	great circle 000/W/23 β = 67 to 090	random scatter	partial great circle 172/E/65	great circle 170/W/20 β = 70 to 080	partial great circle 062/S/80	elongate point maxima - strike ENE-WSW	dextral plunge to NE, sinistral to SE	scatter for dextral kinks. one sinistral kink	a = 63 to 086 b = 25 to 239 c = 10 to 331
31	great circle girdle 005/W/20 β = 70 to 095	-	random or girdle 151/SW/40 β = 50 to 061	great circle girdle 008/E/73	point maxima at 90 to 360 (i.e. vertical)	variable strike, subvertical dips	-	-	four readings, average 62 to 123	four readings, average 114/N/84	a = 72 to 088 b = 13 to 227 c = 12 to 320
32	partial great circle 014/W/25 β = 65 to 104	-	partial great circle 178/W/20 β = 70 to 088	point maxima 69 to 103	point maxima 65 to 090	average plane 085/vert	-	-	one sinistral kink 75 to 075	one sinistral kink 124/NE/85	-
33	great circle 014/W/25 β = 65 to 104	-	point maxima 3 to 340, defines plane 070/S/87	point maxima 65 to 115	three readings, average 62 to 100	three readings, E-W strike, subvertical dip	-	-	-	-	-
34	poorly defined girdle 138/SW/40 β = 50 to 048	-	partial great circle 107/S/15 β = 75 to 017	great circle girdle 079/N/86	great circle girdle 135/NE/77	two readings, average 144/NE/79	two readings, average, 60 to 087	four readings, average, 064/NW/64	dextral kinks, plunge to W and NE	dextral kinks - average plane 014/W/70	a = 65 to 357 b = 5 to 248 c = 26 to 154
35	great circle girdle 168/W/37 β = 53 to 078	-	great circle girdle 013/W/40 β = 50 to 103	point maxima 31 to 099	two readings fall on great circle 142/SW/80	two readings, average 128/SW/28	elongated point maxima 49 to 063	elongated point maxima define a plane 072/S/89	two readings, average 81 to 036	two readings, average 041/SE/78	a = 80 to 250 b = 10 to 078 c = 1 to 342
36	great circle girdle β = 70 to 098	-	great circle β = 50 to 121	point maxima at 50 to 090	-	-	plunge steeply to SE, $B^{S_2}_{So}$ Similar to $B^{S_2}_{S_1}$	AS(So x S_2) Same as AS(S_1 x S_2) NW-SE/ subvertical	plunge variable in NE-SW subvertical plane	dextral average plane 069/N/53 sinistral 093/S/50	-
37	great circle 135/SW/10 β = 60 to 045	-	point maxima at 13 to 323 plane 053/S/77	point maxima 75 to 072	four readings, average 55 to 090	four readings, E-W strike dip subvertical	-	-	-	-	-
38	partial great circle 164/W/15 β = 75 to 074	-	partial great circle 032/W/10 β = 80 to 122	great circle girdle 126/N/86	two readings plunge to NE	two readings E-W strike subvertical dip	two readings plunge to S	two readings average 169/E/67	-	-	a = 60 to 121 b = 18 to 357 c = 23 to 257
39	elongate point maxima or partial girdle	-	random distribution	three points, lie in NE-SW subvertical plane	two readings average 44 to 123	two readings subvertical dip	-	-	-	-	-
40	great circle 062/NW/15 β = 75 to 152	-	partial great circle 016/W/10 β = 80 to 106	partial great circle 015/W/85	two readings average 72 to 235	two readings average 047/E/72	-	-	-	-	-

DOMAIN 25

Nearly all facing evidence indicates that the beds face to the west and hence are overturned, except in minor flexures.

The girdle for bedding defines a β-point which is coincident with the fold axes of the gentle mesoscopic folds observed in the field. The macroscopic trend-line picture (Map 4) shows bedding trending approximately north-south but deformed by gentle warps.

A slaty cleavage is developed in the finer-grained lithologies and has a predominant east-west strike with minor variations in either direction.

The mesoscopic fold axes have orientations similar to those of D2 folds at the localities studied in detail. Since the cleavage does not have an axial plane relationship with these folds it must have formed either before or after them, and must be associated with a macroscopic fold much larger than the size of the domain. The domain possibly occurs close to the hinge of the macroscopic fold because the cleavage intersects the bedding at a high angle.

If the cleavage formed after the mesoscopic folds and is an effect of the last episode of deformation it should occur as subparallel planes defining a distinct point maximum but it forms a partial great circle. This could be interpreted to mean either that the cleavage formed before D2 which then caused the spread of the planes, or that it is fanned. Fanning is not likely because the attitude of the cleavage does not vary systematically from north to south. The bedding must have been planar on the scale of the domain prior to D2 because the great circle girdle is indicative of deformation by plane cylindrical folding.

The picture presented on the synoptic diagram (Fig. II) is the situation for the simultaneous cylindrical folding of two planar surfaces So and S_1 intersecting in a lineation L(So x S_1). So is folded about $B^{S_2}_{So}$ and S_1 is folded about $B^{S_2}_{S_1}$ with both folds sharing a common axial surface (S_2). A similar theoretical situation is described by Turner and Weiss (1963, pp.129-130). The manner in which L(So x S_1) is deformed depends on the mechanism of folding, but in this case the seemingly random pattern is not indicative of a fold mechanism.

It is concluded only that the domain is in the hinge region of a macroscopic D1 fold and has suffered gentle macroscopic and mesoscopic folding during D2.

DOMAIN 26

All bedding from this domain faces to the north or north-west and is upright.

Bedding falls on a partial great circle and β is coincident with fold axes of two gentle mesoscopic folds (hence β = B). The axial surfaces have an average orientation different from that of Domain 25 and similar to that of the D1 folds at the DFL. The cleavage attitude is close to those of the axial surfaces and hence it is considered that this domain mainly shows the influence of D1, rare kink bands being the only evidence of D2. The macroscopic picture indicates that bedding strikes relatively constantly to the NE. It is intersected by S_1 at an angle of about 50° and hence this domain is probably situated on the limb of a macroscopic D1 fold or near the hinge zone if the fold is isoclinal.

DOMAIN 27

All bedding faces to the north or west but most beds dip to the southeast and are overturned. The strike is similar to that in Domain 26 but dips are in the opposite direction.

The β-points for bedding, fold axes and $L(So \times S_1)$ are coincident indicating that they are the effects of D1. One kink fold is the only feature attributable to D2. Mesoscopic D1 folds occur along with overturned bedding having a relatively constant strike. It is intersected by the cleavage at an angle of about 50° and therefore this domain may be on the limb of a macroscopic D1 fold, possibly close to the hinge area.

DOMAIN 28

Numerous sedimentary structures such as flute casts and load casts indicate that the entire sequence in this domain is overturned. Cleavage is rare and insufficient data were collected to determine its orientation accurately but it is tentatively suggested these S_1 may fall on a girdle.

An elongated maximum for axial planes may possibly be explained by fanning of the axial planes of mesoscopic folds associated with a macroscopic fold.

Because β_{So}, β_{S_1} and fold axes are coincident it is considered that this domain has been mainly affected by the D2 deformation and that So and S_1 were planar before the D2 cylindrical folding occurred.

If So, planar in this domain after D1, was part of a D1 macroscopic fold, then when D2 occurred this fold would be deformed about a $B^{S_2}_{S_1}$ axis, and the $B^{S_2}_{So}$ axes, depending on the mechanism of folding, could fall on a great circle. However, because this domain is smaller than the size of the fold, So was planar before D2 and thus produced only $B^{S_2}_{So}$ axes of one orientation. The $B^{S_2}_{S_1}$ axes would not be expected to plot in the same position as $B^{S_2}_{So}$. This situation is very similar to the superposed situation described by Turner and Weiss (1963, p.188, Fig. 5-30c) in which S_1 poles lie on a great circle normal to β_{S_1} and L(So x S_1) lie on a great circle oblique to β_{S_2}.

The synoptic stereographic diagram (Fig. II) indicates that So and S_1 were planar and almost parallel before being cylindrically folded by D2 and hence were on the limb of a macroscopic fold in D1. Trends of So (Map 4) indicate that gentle D2 macroscopic folds as well as mesoscopic folds exist in the domain. The situation is similar to that in Domain 25. So has been folded about β_{So}, and S_1 about β_{S_1}, with both folds sharing the same axial plane S_2. Lineations L(So x S_1) fall on a great circle which enables the mechanism of D2 folding to be determined. Turner and Weiss (1963, pp.478-486) have shown that this pattern is produced where a passive lineation has been deformed by the slip mechanism. The intersection of the L_1 girdle meets the axial plane (the slip plane S_2) in kinematic axis a. The b kinematic axis lies normal to a in the axial plane and hence the kinematic axes of the movement picture can be completely defined. The slip folding of initially planar s-surfaces in So and S_1 has given rise to plane cylindrical folds in So and S_1.

DOMAIN 29

All bedding in this domain is overturned. The dominant pattern exhibited by the girdles of So and S_1 appears to be controlled by the D2 deformation because β_{So}, β_{S_1} and $B^{S_2}_{So}$ are virtually coincident.

Lineations L(So x S_1) form an elongated point maximum or a partial great circle. This is a similar situation to that found in Domain 28 although orientations of the elements are quite markedly different.

The synoptic diagram indicates that So and S_1 were refolded about β_{So} and β_{S_1} respectively. The great circles indicate cylindrical folding of an originally planar surface, although variations from the great circles exhibited particularly by So suggest small areas were non planar before D2.

This is supported by the presence of rare D1 mesoscopic folds. The $B^{S_2}_{So}$ and $B^{S_2}_{S_1}$ fold axes should fall in the axial plane S_2 and here define a plane 340/E/71 which varies slightly from the pattern listed in Table 8.

Because L(So x S_1) defines a great circle it indicates that D2 has been folded by the slip mechanism. The kinematic axes can be determined and the movement picture will be discussed later.

Macroscopic trend lines indicate that So and S_1 intersect each other at an angle of up to 60° indicating location of the domain on the limb of a D1 macroscopic fold, possibly near the hinge zone.

DOMAIN 30

This domain consists of well bedded sediments, which all appear to be overturned. Poles to bedding define a great circle but a scattering of points away from the girdle indicates that So was not entirely planar before being folded about the β-point.

Cleavage, S_1, defines a great circle and hence a β-point which is the fold axis about which S_1 has been folded. Numerous mesoscopic folds have a style similar to the D1 folds in the Balaclava Stream Locality (p. 70-71). The axial surfaces of D1 folds define a great circle which is almost coincident with the So and S_1 girdles indicating that before D2 the So and S_1 were virtually planar and parallel indicative of a situation on the limb of a macroscopic D1 fold. Mesoscopic D1 folds were the cause of minor inconsistencies in the planar So and account for the scatter around the ΠSo girdle.

$B^{S_2}_{So}$ fold axes define a partial great circle which is the axial plane (S_2) in which the fold axes lie. The great circle occurs as a result of deformation of a non-planar form surface. This situation is similar to that illustrated by Turner and Weiss (1963, Fig. 4-33) for the superposition of two systems of plane folds where S_1 and $B^{S_1}_{So}$ belong to one system and S_2 and $B^{S_2}_{So}$ belong to the other system. The great circle for Lo and $B^{S_1}_{So}$ indicate that D2 folding was by the slip mechanism. The kinematic axes can be determined, and the movement picture will be discussed later.

DOMAIN 31

Facing evidence indicates that sediments in an area on both sides of the Lock Creek Locality (p.69) are upright but further upstream and

downstream these sediments are overturned. Cleavage is rare in this domain, the sediments being predominantly silty and sandy.

D1 mesoscopic folds have axial surfaces with a scattered pattern that may result from later effects of D2 or from fanning of mesoscopic folds on a macroscopic fold. The domain exhibits the effects mainly of D1, but evidence of D2 is offered by the $L(So \times S_1)$ and S_1 great circle patterns and by minor kink folds.

Macroscopic folds occur in the area, as shown by an area of upright bedding in between overturned beds. Using the axial plane of D2 folds of the locality within this domain that was studied in detail (Fig. 54) the kinematic axes can be determined because $L(So \times S_1)$ define a great circle and hence have been deformed by slip folding.

DOMAIN 32

All bedding in this domain appears to be overturned. Poles to bedding define a β-point about which the bedding has been folded. The poles to cleavage define either an elongated point maximum possibly due to axial plane fanning, or more probably a partial great circle defining a β-point about which the cleavage has been gently folded on the macroscopic scale, the only mesoscopic evidence for D2 being kink bands.

Because of the constant orientation of $L(So \times S_1)$ it is obvious that this area exhibits only the influences of the D1 deformation. D1 axial surfaces have almost vertical dips and strike approximately east-west. This area is possibly close to the nose of a macroscopic D1 fold because bedding and cleavage intersect at almost 90°.

DOMAIN 33

This domain consists of a macroscopic fold in So, the hinge area or one limb of which appears to consist of upright bedding while the bedding in the remainder of the domain is overturned. There are mesoscopic D1 folds. A macroscopic fold appears to be a large scale D2 kink fold having a shear zone coincident with the axial surface.

DOMAIN 34

This domain includes the "Fossil Locality" (pp.71-72). One small area between two dykes, and part of the "Fossil Locality", have upright

bedding, the remainder of bedding being overturned. The synoptic stereographic projection illustrates a complex geometrical picture. The deformed lineations L(So x S_1) and $B_{So}^{S_1}$ fall on great circles of differing orientations indicating that they must have had differing orientations before the D2 folding. These D1 lineations would define two kinematic axes for the movement picture. However, the spread of L(So x S_1) is considered to be a result of one of the processes listed in Chapter 2 (pp.46-47) and the $B_{So}^{S_1}$ girdle is the significant one. The kinematic axes can be determined, and a slip mechanism of deformation is suggested by the data.

DOMAIN 35

In the southern part of this domain bedding has a relatively constant orientation but changes from upward facing to overturned at least twice suggesting the possible presence of almost isoclinal macroscopic folds. For the remainder of this domain the bedding is overturned.

The dominant mesoscopic folds are of the D2 generation, their axial surfaces being defined by an elongated point maximum or a partial great circle girdle. This is possibly due to fanning of the mesoscopic axial planes associated with a macroscopic fold.

The synoptic stereographic projection indicates that the kinematic axes can be determined. However due to the paucity of data on D1 folds any results are considered very tentative. The machanism of D2 is deformation by slip folding.

DOMAIN 36

All bedding observed is overturned. The most complex structures of the Rockvale region occur in this domain. The D1 axial-surface slaty cleavage is in tight chevron folds. All mesoscopic folds are of the D2 generation. The D1 folds were on a scale larger than the outcrop scale but two relict macroscopic folds (a synclinal antiform and an anticlinal synform) were observed. Cleavage defines a great circle indicating that D2 produced cylindrical folds.

D2 fold axes in bedding ($B_{So}^{S_2}$) and in cleavage ($B_{S_1}^{S_2}$) exhibit a similar pattern. In this domain kink bands, particularly in the cleavage,

are extremely well developed with both dextral and sinistral types occurring. The attitudes of the kink planes of the two types vary significantly but the fold axes tend to be markedly similar indicating that the kinks form conjugate pairs, similar to those illustrated by Ramsay (1967, Fig. 7-126).

The method of Ramsay (1962b) for determining the orientation of the principal axes of stress was used to determine σ1, σ2, σ3 for five sets of conjugate kink bands. σ2 occurs at the intersection of the two kink planes, σ1 here forms the obtuse bisectrix of the two kink planes lying in or very close to the unrotated foliation, and σ3 is normal to σ1 and σ2. The greatest principal stress axis is oriented at approximately 8 to 215. It has been suggested that strong development of conjugate kinks may lead to the formation of chevron folds (Paterson and Weiss 1966), and that complete transformation of conjugate kinks to chevron folds would require a compressive strain of 50%. Because of the presence of well developed chevron folds in this domain (Plate 13) along with the kink folds it is obvious that the chevron folds have developed from the transformation of kinks.

DOMAIN 37

On facing evidence all bedding is overturned. This domain exhibits influences of mesoscopic D1, the only effects of D2 being observed in the ΠSo net and gentle flexuring of this feature (see Map 4).

A summary of the structure of the domains on this scale is included in the discussion of the Rockvale area macroscopic structure at the next larger scale.

C. Medium Macroscopic Scale

The main detailed work at this scale was done in the Rockvale area although data from the Aberfoyle, Herbert Park and Wollomombi areas (Domains 38-40) were collected as a check of structural consistency throughout the block.

ROCKVALE REGION

The overall picture of the Rockvale area from interpretation of domains 25-37 and maps of the regional trends of mesoscopic structures is

that the area is dominated by a large fold (here termed the Rockvale Anticlinal Synform) plunging steeply to the east. The axial surface, which is parallel to the regional strike of cleavage, is subvertical striking east-west and passing through the isoclinal fold locality near the crossing of Rockvale Creek (GR 4990 2406) and thence just to the north of the "Double Fold Locality". A three dimensional interpretation of the structure is given in Figure 62 which covers the area of domains 25-36.

Minor warping and variation in the strike of So is considered to be a result of D2, which also produced the S-type fold in Boundary Creek (illustrated as inset on Figure 62). The axial surfaces of the S-type fold, which occurs on the northern limb of the Rockvale Anticlinal Synform, show very prominently as two lineaments on aerial photograph NSW 299-5601, but on the ground appear as minor shear zones which normally will be regarded as insignificant.

Synopsis of Rockvale region

The data illustrated for Domains 25-37 (Fig. II) can be grouped so that folds of the same generation fall together. For domains affected by D2 the β_{So} ($= B^{S2}_{So}$) intersections define a weak partial great circle girdle and S_2 are virtually coplanar. Intersections of S_2 define β_{S_2} but these are not fold axes (Fig. 63).

For domains affected by D1 the β_{So} ($= B^{S1}_{So}$) intersections are almost coincident forming a cluster (Fig. 63A) of points. The axial planes apart from those in Domain 26, are coincident (Fig. 63B), and a very weak β_{S_1} axis (a fold axis B^{S2}_{S1}) is defined lying in the B^{S2}_{So} great circle (Fig. 63C). The B^{S2}_{So} great circle should coincide with the S_2 planes (Fig. 63D) and the variation here is difficult to explain unless the second period of folding was nonplane.

In conclusion, the Rockvale area has been affected by two periods of folding:

D1. Plane cylindrical folding about an axis (B^{S1}_{So}) which initially was probably plunging steeply to the east. Plane cylindrical segments of this first period of folding have been preserved in scattered domains (26, 27, 32, 35, 37). The cylindrical form is demonstrated by the great-circle patterns for So and the initial planar form is demonstrated by the cylindrical folding of the axial planes in the later period of folding.

D2. Plane noncylindrical folding about B^{S2}_{So} axes of variable orientation

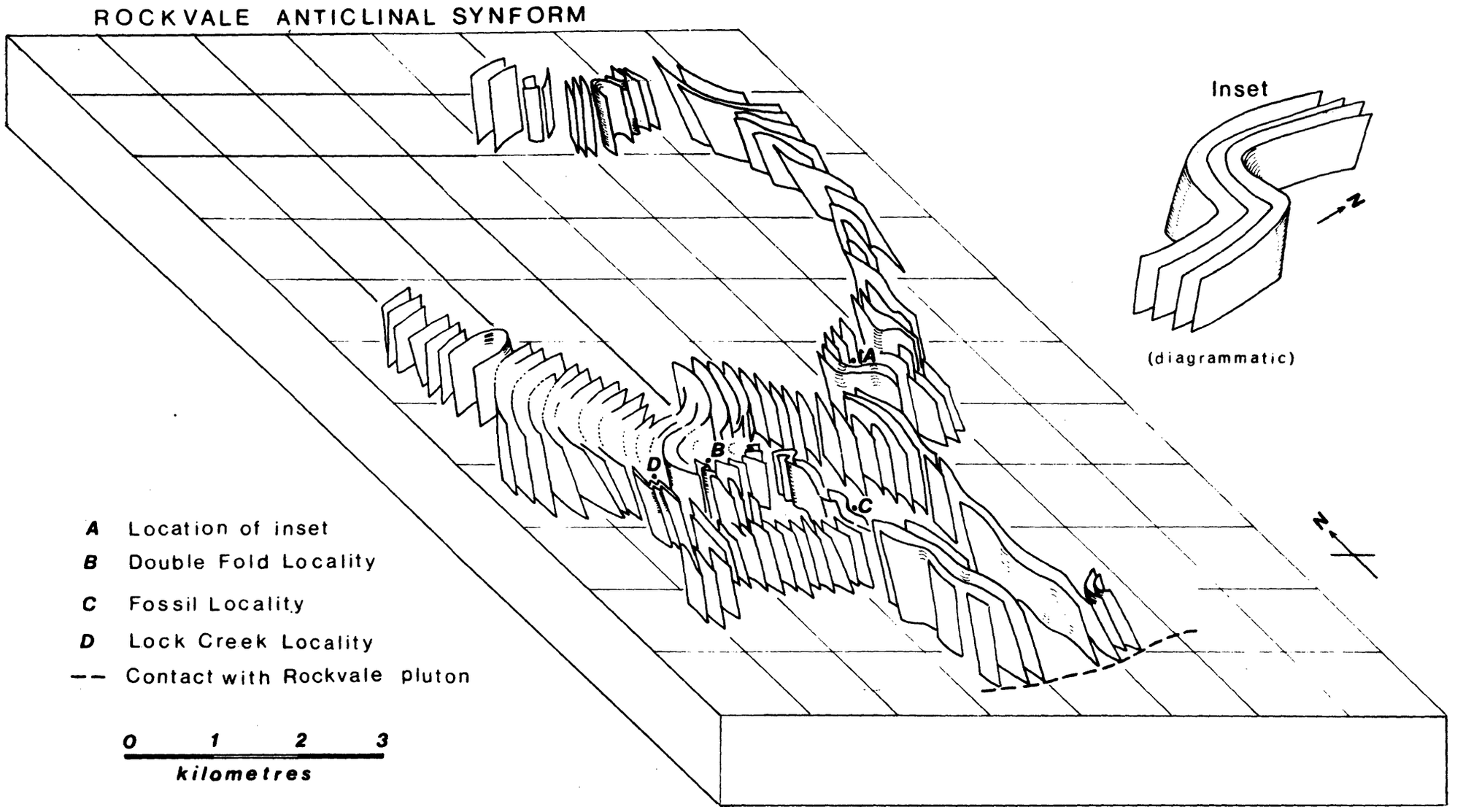

Fig. 62: Diagrammatic form surface representation of the Rockvale anticlinal-synform and surrounding sediments of the Rockvale area.

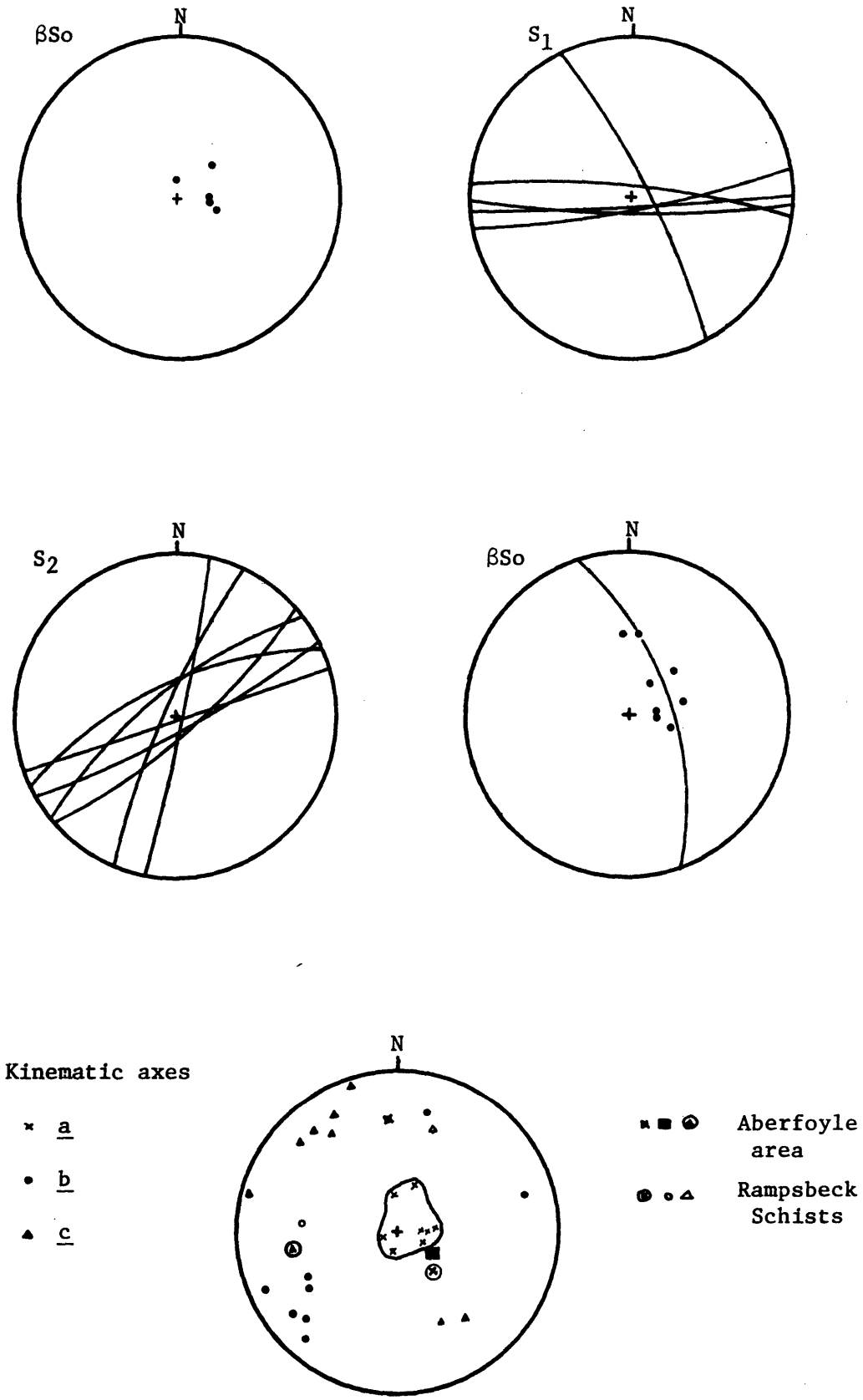

Fig. 63: Synoptic stereographic projections and Kinematic axes for domains from the Rockvale Block.

which define a great circle girdle which is not parallel to S_2. The domains other than those listed above contain segments of So that were effectively planar after D1, and in them cylindrical $B_{So}^{S_2}$ folds formed during D2 having axial planes striking approximately NE.-SW. with subvertical dips.

In several domains it has been possible to determine the kinematic axes during the D2 episode of folding (see Table 8). The axes are remarkably consistent over the Rockvale area: a is subvertical, b plunges shallowly in a NE.-SW. plane, and c plunges shallowly to the NW. or SE. (see Fig. 63E). Because lineations produced by D1 define a great circle girdle due to D2, the D2 episode has produced folds by the slip mechanism (probably the flow variety).

The axes of D2 folds ($B_{S_1}^{S_2}$) have no unique kinematic significance. They are generally inclined to both the a and b kinematic axes and have not been observed to coincide with b. The D2 slip (or flow) folding of the initially planar s-surfaces (S_1) has given rise to plane cylindrical folds in S_1 whereas this folding of the initially curved and folded So surfaces has given rise to plane noncylindrical folds.

ABERFOYLE AREA (DOMAIN 38)

This domain is located mainly north of the Guyra-Ebor road and consists of the Girrakool Beds west of the Glen Bluff Fault. Facing evidence, where observed, suggests that all bedding is overturned although this situation may change with future detailed mapping. The stereographic projections (Fig. II) suggest that two periods of folding have occurred. The first folded So producing an axial plane slaty cleavage and an $L(So \times S_1)$, and the second deformed S_1 and $L(So \times S_1)$, the mechanism being slip (or flow) folding.

Two closed folds (interlimb angles 40 and 77) plunge steeply to the northeast and have steeply dipping axial surfaces striking approximately east-west. By contrast, two gentle folds from a separate locality (interlimb angles 135 and 152) plunge steeply towards the south and have steeply eastward dipping axial surfaces striking approximately northsouth. It is considered the closed folds are of the D1 generation and the gentle folds are of D2. Assuming an average axial plane of 169/E/67 for D2 folds the kinematic axes can be determined (see Table 8). When plotted with the kinematic axes for the Rockvale domains (Fig. 63E) a close similarity in the a axis is noticeable, supporting the observations that the Aberfoyle Domain

has been affected by two periods of mesoscopic deformation similar to those at Rockvale.

HERBERT PARK AREA (DOMAIN 39)

This domain is located in the southwest corner of the field area and contains both upright and overturned bedding, but insufficient data have been collected to warrant any other conclusions. Lewis (1973) working to the west of the field area around the Puddledock - Gara River area examined the Girrakool Beds along the Gara River and found most of the beds to be overturned. He provided a composite plot of 32 mesoscopic fold axes which define two partial great circle girdles of attitudes 140/NE/70 and 052/SE/70. These correlate respectively with D1 and D2 folds in the Rockvale district and consequently it is concluded that this area has suffered the same deformations as the Rockvale area.

WOLLOMOMBI AREA (DOMAIN 40)

This domain is located in the southern part of the Rockvale Block and contains both upright and overturned bedding. Simandjuntak (1974) studied a small area within a radius of 1.5 km of Wollomombi Village and found bedding in general to be upright, with minor local overturning.

Dun (1964) and Simandjuntak (*op. cit.*) working in the same small area, described mesoscopic isoclinal folds and interpreted the macroscopic structure as consisting of isoclinal folds with rounded to sharp hinges. Dun concluded that the area had been affected by two periods of deformation. Simandjuntak concluded that the area had suffered only one deformation, but he presented plots showing S_1 defining a great circle which he explained by axial surface fanning. The data presented here for $L(So \times S_1)$ indicate that S_1 and L_1 have been folded by a second period of deformation. Hence this domain is similar to the remainder of the Rockvale Block.

RAMPSBECK SCHISTS (DOMAIN 41)

This domain is wholly within the Rampsbeck Schists (Map 3). Data presented (Fig. 64) include readings collected by two undergraduate students (Fisher 1968, Perkins 1968) as well as those collected by the writer. Bedding is rarely recognisable and, apart from rare amphibolite bands, is discernible only as a colour change in the schists. S_1 is represented by

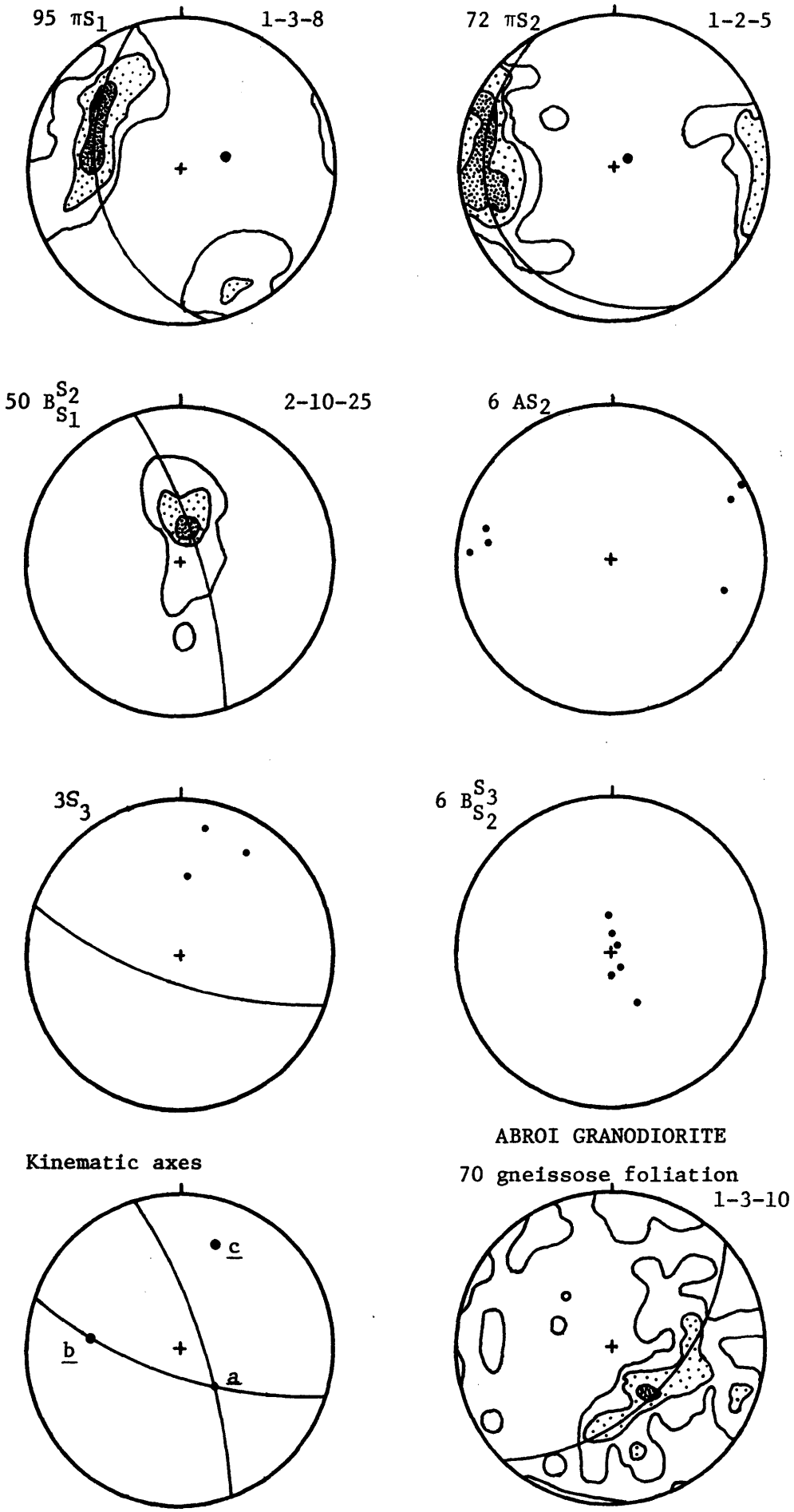

Fig. 64: Stereographic projections for the Rampsbeck Schists and Abroi Granodiorite.

a well developed schistosity penetrative on the scale of the outcrop, and ΠS_1 defines β_{S_1} = 55 to 075 ($=B^{S_2}_{S_1}$). Mesoscopic folds in S_1 have steeply plunging fold axes which define a partial great circle girdle oriented at 162/E/75. Axial surfaces for these folds are parallel to an S_2-schistosity that is confined to the higher grade schists. S_1 is commonly observed being transposed into S_2. The axial surfaces to the $B^{S_2}_{S_1}$ folds strike north-south with subvertical dips. ΠS_2 defines a partial great circle indicating gentle folding after the formation of S_2, and β_{S_2} = 80 to 062.

Folds in S_2 occur as gentle flexuring of the schistosity about an east-west striking axial surface (S_3) which results in deviations of up to 40° from the main north-south strike of S_2. $B^{S_3}_{S_2}$ fold axes are steeply plunging to subvertical. Using an average axial surface (S_3) of 108/S/68 the kinematic axes for D3 can be defined as: $\underline{a}$ = 54 to 140, $\underline{b}$ = 28 to 276, $\underline{c}$ = 22 to 018. The significance of these will be discussed later.

ABROI GRANODIORITE (DOMAIN 42)

This domain consists of the Abroi Granodiorite south of the Guyra-Ebor road. The pluton is marked by a well developed gneissic foliation resulting mainly from the preferred orientation of biotite flakes. As well as data collected by the writer the Π-plot of foliation (Fig. 64) also includes some data collected by Collerson (1967). There is a partial great circle with β = 44 to 316. This is similar to the orientation of bedding immediately west of the intrusion in the Wollomombi area where Dun (1964) found macroscopic D1 folds with a fold axis of 78 to 324.

Binns (1966) and Leitch (1972) considered that the foliation is the result of primary flow of the magma, and Leitch found also that the S_1 cleavage in the Styx River Beds is conformable with the gneissic foliation in the granodiorite. Consequently he considered it likely that both developed during the D1 deformation episode.

Xenoliths are abundant in the granodiorite and tend to be aligned in the foliation which occasionally wraps around the xenoliths (Binns 1966, p.17; Leitch 1972, p.274). However in some places (e.g. GR 5235 2375) a very distinct foliation is seen cutting the xenoliths angles up to 20° and consequently this foliation is considered to represent a later foliation formed during D2 and cutting the original primary flow foliation which developed during D1. Hence the Π-plot of foliations may contain foliations of two episodes which have not been distinguished in the field because of

their similar orientations. Binns (1966) described xenoliths transvere to the foliation which in some cases wraps around the xenolith and in others continues without change of orientation up to the xenolith margins.

The Abroi Granodiorite has suffered considerable cataclastic deformation (Binns *op. cit.*) although Leitch (*op. cit.*) failed to recognise any cataclasis in hand specimens from the southern portion of the pluton. In places (e.g. near Wongwibinda Fault at Riverview) the cataclastic foliation is inclined to the primary foliation at an angle of 30° but generally the two foliations are parallel (Binns *op. cit.*, p.8). Simandjuntak (1974) described a flow foliation (S_1) and a later shear foliation (S_2) which are essentially parallel, in the southern portion of the pluton near Wollomombi Village.

D. Large Macroscopic Scale

The gross structure of the Rockvale Block is examined this scale. The Block contains the effects of two tectonic deformations with all rocks showing the effects of at least one episode.

The effects of D1 are mainly observed in the relatively unmetamorphosed sediments which occur in the north, west and southern parts of the block. D1 has produced folds which range in tightness from open to almost isoclinal and have an associated axial-surface slaty cleavage. The folds range in size from mesoscopic (hand specimen) to macroscopic with the Rockvale Anticlinal Synform occupying an area of 3 km x 5 km. Dun (1964) inferred D1 macroscopic folds approximately 2 km x 2 km in sediments at Wollomombi. Initially the D1 folds probably had fold axes plunging steeply to the east and subvertical east-west striking axial surfaces. In the east of the Rockvale Block in the Wongwibinda Complex the effect of D1 is barely recognisable, traces of bedding are rarely seen, B_{So}^{S1} folds are not observed and the slaty cleavage has, with increased metamorphism, changed to a penetrative schistosity.

The Abroi Granodiorite appears to have been emplaced immediately before, or during, the D1 episode because the flow foliation in it is parallel to the strike of the schistosity in the north, and defines a great circle in the south as do D1 macroscopic folds in So. The Rockvale Adamellite-Granodiorite varies from massive to foliated. Because of alignment of xenoliths the foliation appears to be a primary flow structure oriented east-west parallel to the slaty cleavage in the sediments. Hence

the Rockvale pluton was possibly intruded during D1.

The D2 episode of deformation caused folds in the low-grade metamorphosed sediments with variable steeply plunging axes and subvertical axial surfaces which strike approximately NE.-SW. These folds vary considerably in style from gentle warps on limbs of D1 folds, through kink bands to tight chevron folds in the slaty cleavage. They also vary in size from microscopic to macroscopic. The macroscopic S-type fold in Boundary Creek (Fig. 62, inset) has one axial surface represented by a shear surface.

In the Wongwibinda Complex the effects of D2 are noticeably different from those in the western portion of the Rockvale Block. S_1, represented by a penetrative schistosity, has been rotated from an east-west to a north-south orientation, and transposition of S_1 to S_2 has occurred in the high-grade schists. $B_{S_1}^{S_2}$ folds differ in style from those observed in the Girrakool Beds and are commonly isoclinal with the limbs often being transposed into S_2.

The rotation of the orientation of S_2 from NE.-SW. to NNW.-SSE. has probably resulted also in the rotation of the b and c kinematic axes determined in the Aberfoyle area and in the Rampsbeck schists. Binns (1966) visualised the swing in S_1 through 120° as a gigantic drag due to sinistral movement on the Wongwibinda Fault. This possibility will be discussed later.

A late stage minor deformation, D3, has occurred resulting in a slight swing in strike of S_2 in some outcrops, and it is considered to be a waning phase of D2.

Dykes and Macroscopic Faults

DYKES

Numerous dykes occur throughout the Rockvale area (Fig. 65) and vary in composition from porphyritic acid types to hornblende lamprophyres. They have a mean orientation of 061° indicating they have been preferentially emplaced along northeast-southwest trends, which is the orientation of the second deformational episode. Hence the dykes are a late stage event in the history of the Rockvale Block.

FAULTS

Wongwibinda Fault: The Rockvale Block is bounded on the east by this fault which has been described in detail by Binns (1966). The fault has sheared

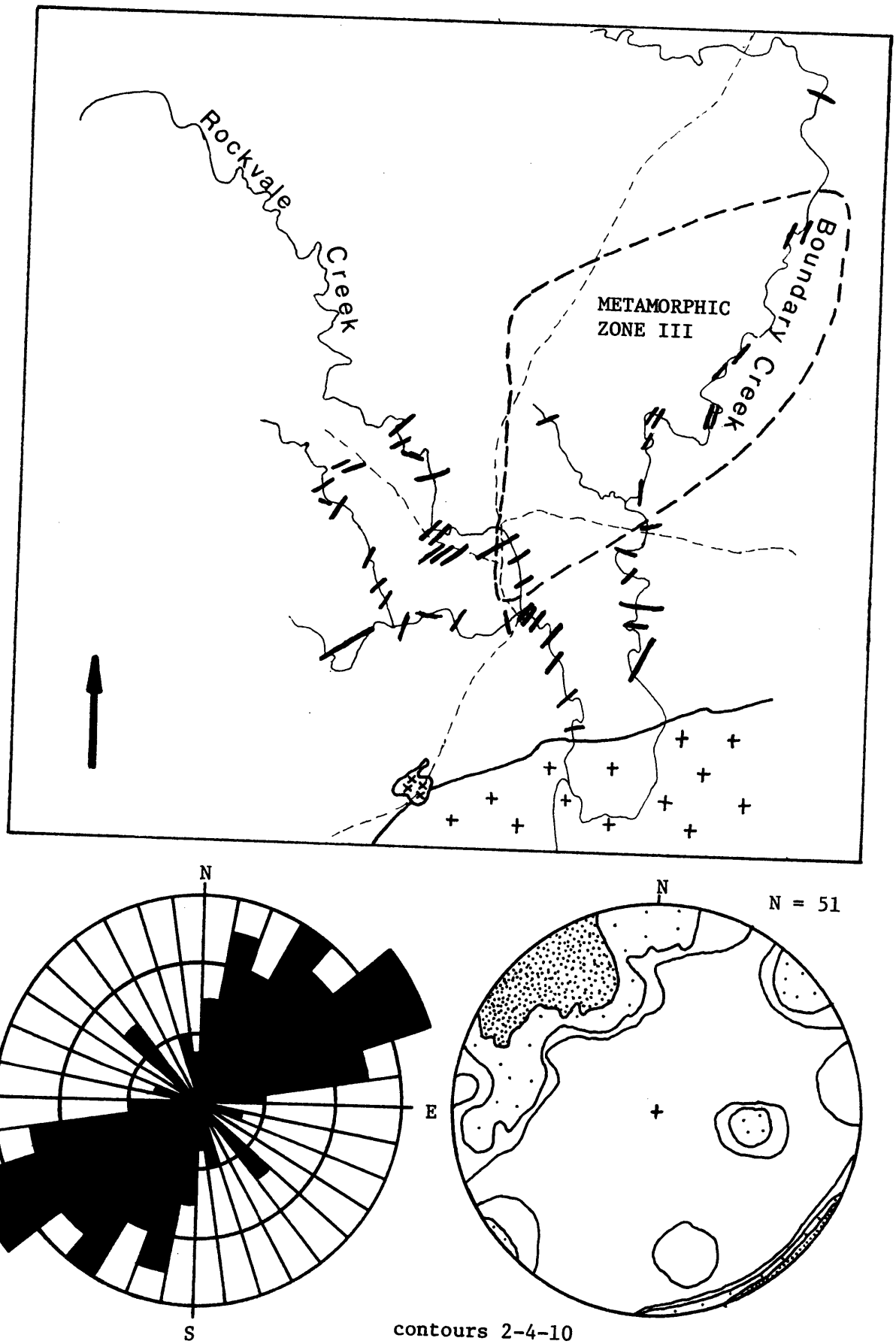

Fig. 65 A: Location of dykes in the Rockvale region.

B: Rose diagram for strike of dykes. Spacing for concentric circles is two readings.

C: Stereographic projection for orientation of the dykes.

the Abroi Granodiorite and Dyamberin Beds and produced a mylonite in the fault surface. The cataclastic foliation is generally parallel to the primary flow foliation but in places the two foliations intersect at angles up to 20°. South of Wongwibinda the fault dips steeply to the west but further north flattens out to dip west at about 35°. Binns (*op. cit.*) claimed that five separate phases of movement occurred, the first in Permian time and the last in the Tertiary.

The present writer considers that all the phases of movement of Binns including transcurrent movement, near vertical movement and reverse movement could possibly be accounted for by one main period of movement which took place over an extended period of time. The Tertiary period of movement was proposed by Binns because there is a difference in the base levels of Tertiary basalts of 300-500 feet. However, the necessity to invoke faulting is doubted or denied because Collerson (1967) has described over 300 feet in local relief before the basalt outpourings in the Doughboy Range immediately west of the Wongwibinda Fault, and Binns (*op. cit.*) also estimates the prebasalt relief to have been 500-1000 feet.

It is clear nevertheless that the Wongwibinda Fault has been an important structure asserting a major influence on the Rockvale Block in Permian time, as will be discussed later.

Chandler Fault: This fault was mapped by Binns and others (1967) and its position modified by Leitch (1972) and Simandjuntak (1974). It occurs on the southern side of the Abroi Granodiorite and is truncated by the Round Mountain Leucoadamellite. To the southwest, outside the field area, the fault truncates the eastern end of the Hillgrove Adamellite.

The fault dips steeply to the north and has sheared the granodiorite producing mylonites similar to those along the Wongwibinda Fault. It is tentatively suggested here that the Wongwibinda and Chandler Faults are the same structure truncating the southern and eastern edges of the Abroi Granodiorite.

Fishington Fault: Activity along this vertical fault was confined to a relatively short period during the Permian because it displaces the Wongwibinda Fault and is truncated by the Glen Bluff Fault. Binns (*op. cit.*) considered that either a vertical movement of over 5200 m of the north block or a sinistral strike-slip movement of over 3000 m is needed to explain the dip-separation and strike-separation on the Wongwibinda Fault. For want of

recognition of piercing lines, the true dip-slip and strike-slip components of the slip on the fault cannot be measured at present.

Glen Bluff Fault: This fault is the youngest major structure in the Rockvale Block, truncating the Fishington Fault and being intruded by the Wards Mistake Adamellite. It is subvertical, is marked by cataclasis in granitic rocks, and to the south is marked by a zone of shearing up to 150 m wide. Collerson (1967) and Perkins (1968) found no evidence to suggest that this fault extends as far as the Abroi Granodiorite. It appears to die out approximately 1.5 km north of the intrusion.

Apart from cutting the Tobermory Adamellite the Glen Bluff Fault marks the western extremity of thoroughly recrystallised Rampsbeck Schists and their contact with the zone of Transitional Schists (see Appendix I, p.82).

MECHANISMS FOR OVERTURNING THE GIRRAKOOL BEDS

In the Rockvale Block a major problem, discussion of which has been avoided until now, is an explanation of the overturning of the majority of sediments in the Girrakool Beds. Small areas around Rockvale have upright bedding but although the bedding dips in opposite directions the facing evidence indicates that the upright and overturned portions both young (or face) in the same direction (usually towards the west). Consequently it is considered that the whole region was overturned and that later warping by one of the mechanisms discussed for the Coffs Harbour Block (p.50) has altered the dips of some of the sediments so that they now appear upright.

Several hypotheses can be suggested to explain the overturning:

1. Large scale macroscopic folding to produce folds with one limb overturned. One fold style might have been a tight to isoclinal asymmetrical fold with one limb overturned. The area of overturning includes the Aberfoyle, Herbert Park and Wollomombi regions and on this scale the macroscopic fold must have one limb covering an area of at least 25 km x 30 km. The Girrakool Beds do not extend much further than the field area being examined here and the upright limb for this isoclinal fold has not been found. It may be possible that the mainly upright Carboniferous Sandon Beds described by Smith (1973) west of Armidale represent the upright limb of this fold. However the geometry of the

Sandon Beds is confused by at least two periods of mesoscopic folding and no concrete evidence for that area being the limb of a macroscopic fold was found.

2. The overturning may be the result of a nappe, possibly associated with thrust faulting. In most cases where thrusting has produced nappes the large part of the thrusted sheet, both upright and overturned, has a subhorizontal orientation. To produce the situation observed in the Rockvale Block either the upright limb has been removed by erosion, or a thrust has removed the upright material exposing the overturned material. No evidence has been found to suggest a low angle thrust fault and because the majority of bedding has dips steeper than 45° it is considered that the overturning is unlikely to have been produced by nappes or thrust faulting.

3. The overturning may possibly be explained by effects of strike-slip faulting, similar to that proposed by Lillie (1962b) and Grindley (1963) to produce subvertical bedding and steeply plunging folds in the southern Alps of New Zealand. Waterhouse (1972) attributed these steeply plunging folds to originate by tectonic thickening producing steeply dipping schuppen followed by two periods of folding. Waterhouse attributed this folding to have taken place under the influence of a strike-slip regime which was operating in a subduction zone. In New Zealand the majority of bedding is upright with only slight overturning possibly due to the tight folding.

   Up to the present time no major strike-slip faults have been recognised in New England although with future work it is possible that the Peel Fault or the Demon Fault or both may turn out to be important strike-slip faults. Because of the failure to recognise this type of fault in New England it is considered that the overturned material at Rockvale was not produced by this method.

4. The overturning of the Rockvale sediments may have been caused by intrusion of granitic plutons. A theory for diapirism and structures produced by diapirs has been developed by Ramberg (1967a), Stephansson (1972) and Berner *et al.* (1972) and is supported by centrifuged and non-centrifuged models (e.g. Ramberg 1963, 1967b, 1970, 1972; Stephansson 1971). Field evidence has been produced by Bridgewater *et al.* (1974) and O. Stephansson (pers. comm.).

   Ramberg (1967a, pp.53-58 and 87-92) has outlined the geometric features

of domes generated by gravity. Ramberg has shown that during the late stages in domal development a mushroom shape occurs (Ramberg, Fig. 30A) and during this period overturning of the layering in the overburden adjacent to the upper parts of the dome is a typical geometric feature. The overturning is due to drag by the rising and laterally flowing mass. O. Stephansson (pers. comm.) considers that overturning of overburden can occur even before the diapiric pluton has reached the mushroom stage.

Using the centrifuged model of Ramberg (1967a, Fig. 35) the overturned material extends a distance of more than 2.5 times the thickness of the trunk of the diapir, dips towards the intrusion but youngs away from the intrusion. When applying this model to the Rockvale Block it can be seen that the overturned beds occur in a zone which is at a distance up to approximately 2 times the thickness of the Abroi Granodiorite from the contact. The beds generally dip towards the contact and face in the opposite direction. Hence it is considered that while the Permian Girrakool Beds were in a mobile state they were intruded by the Abroi Granodiorite as a dome which possibly caused the overturning of a large volume of sediment now found around Rockvale.

AGE OF THE DEFORMATIONS AND RELATION TO METAMORPHISM

Limited fossil evidence from the Girrakool Beds and Dyamberin Beds indicate that at least part of these formations were deposited in Permian time (see Appendix, pp.8-10). K-Ar ages have been determined by Binns and Richards (1965) for units of the Wongwibinda Complex and associated granitic rocks and a summary of the geological history of the Wongwibinda district has been provided by Binns (1966, Table 7). The summary of Geological events presented here (Table 9) differs markedly from the earlier interpretation of Binns (*op. cit.*).

Previous workers have divided the granitic rocks of New England into three suites (see Appendix, p.89 and Table 16). Plutons representing the Hillgrove Suite occur in the Rockvale Block and representatives of the New England Batholith *sensu stricto* border the block (see Map 1.). K-Ar ages listed by Binns and Richards (1965) for the Abroi Granodiorite are 252 m.y. and 259 m.y. for the Tobermory Adamellite. Binns (1966) appears confused in that he considers field evidence shows the Tobermory Adamellite intrudes the Abroi Granodiorite and consequently must be younger (p.24). However

Table 9: Summary of Geological events in the Rockvale Block

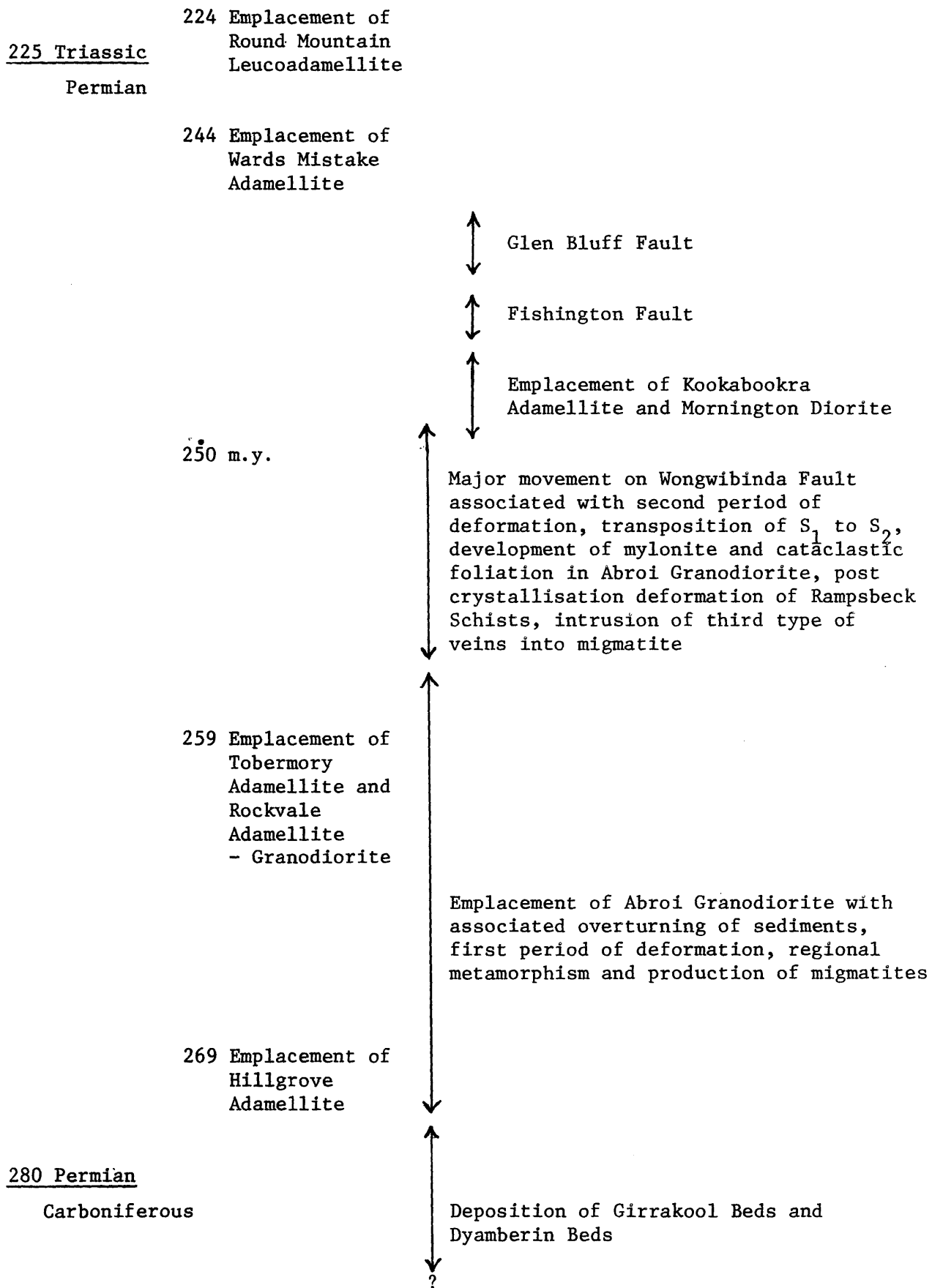

later (p.27) Binns regards the Abroi Granodiorite as being the last intrusion in the sequence of Hillgrove-type plutons.

Contrary to Binns (*op. cit.*) the Abroi Granodiorite appears to be one of the first plutons to be intruded into the Rockvale Block. The primary flow foliation seen in the southern part of the intrusion appears to be folded around a fold axis similar to that observed in the sediments. This suggests that the Abroi Granodiorite was either emplaced before the onset of the first period of deformation or during the early stages of the deformational episodes.

It is considered here that the emplacement of the Abroi Granodiorite (a syntectonic pluton) has resulted in the overturning of a large portion of the Girrakool Beds, and is associated with the D1 deformational episode, the regional metamorphism which produced the Rampsbeck Schists and the development of the Zone of Migmatites. A close association between the deformation and metamorphism is indicated by the development of the slaty cleavage in the Girrakool Beds which becomes the schistosity in the Rampsbeck Schists.

The majority of the above events must have been completed prior to 259 m.y. because the Tobermory Adamellite intrudes the granodiorite and migmatites. The Rockvale Adamellite-Granodiorite is considered to have been emplaced at this time. Both intrusions have a weakly developed foliation and therefore D1 must have been still operative at this time.

Binns and Richards (1965) list K-Ar ages for the Rampsbeck Schists (250 m.y.), Abroi Granodiorite (252 m.y.) and Zone of Migmatites (253 m.y.). The present writer accepts these ages but seriously doubts the interpretation of the events at this time by Binns (1966). The following interpretation is preferred. Around 250 m.y. major movement occurred on the Wongwibinda Fault associated with the second period of deformation and produced the transposition of S_1 into S_2, the mylonite in the fault plane and the cataclastic foliation in the Abroi Granodiorite. The K-Ar ages of Binns and Richards (*op. cit.*) can be explained as follows:

(i) Abroi Granodiorite 252 m.y. The Abroi pluton has suffered considerable cataclastic deformation and is rarely free of dislocational effects (Binns, 1966, p.17). Hence this date of 252 m.y. is for the age of the cataclasis and not the age emplacement or cooling.

(ii) Migmatite Zone 253 m.y. The vein dated by Binns and Richards is one of Binns' (1966, p.15) youngest veins (Type 3) and indicates that the migmatisation process extended over a long period of time from prior to 259 m.y. to at least 253 m.y.

(iii) Rampsbeck Schists 250 m.y. This specimen was collected by Binns from the high grade zone where transposition of S_1 into S_2 has occurred. Binns (*op. cit.* p.14) has indicated that localised post-crystallisation deformation of the schists has occurred and K-feldspar has been replaced by muscovite or myrmekite. Consequently there has been probably loss of radiogenic argon from the biotites at this time. This is a similar situation to that described by Mason (1961) in the New Zealand Alps where schists close to the Alpine Fault have been dated at less than 10 m.y. by K-Ar methods. On geological evidence the time of metamorphism was early Cretaceous or older. Mason postulated argon loss due to deep burial which kept the temperature above the limit for argon retention.

Binns (*op. cit.*) considers the 250 m.y. ages date the closing stages of the regional metamorphism of the Wongwibinda Comples but for reasons outlined above it is here considered that the 250 m.y. ages date the cessation of the second period of deformation and associated movement on the Wongwibinda Fault.

Towards the end of the movement on the Wongwibinda Fault the Kookabookra Adamellite and Mornington Diorite were emplaced. Movement then occurred on the Fishington Fault followed by movement on the Glen Bluff Fault.

All deformation, metamorphism and fault movement had finished prior to the emplacement of the post-tectonic Wards Mistake Adamellite at 244 m.y. and the Round Mountain Leucoadamellite at 224 m.y.